J. Fluid Mech. (2006), *vol.* 563, *pp.* 319–355.
doi:10.1017/S002211200600125X Printed in the United Kingdom

The stability of two connected drops suspended from the edges of circular holes

By LEV A. SLOBOZHANIN AND J. IWAN D. ALEXANDER

Department of Mechanical and Aerospace Engineering and National Center for Space Exploration Research, Case Western Reserve University, Cleveland, Ohio 44106, USA

(Received 21 June 2005 and in revised form 23 February 2006)

The stability of an equilibrium system of two drops suspended from circular holes in a horizontal plate is examined. The drop surfaces are the disconnected axisymmetric surfaces pinned to the edges of the holes. The holes lie in the same horizontal plane and the two drops are connected by a liquid layer that lies above the plate. The total liquid volume is constant. For identical pendant drops pinned to holes of equal radii, axisymmetric perturbations are always the most dangerous. The stability region for two identical drops differs considerably from that for a solitary pendant drop. A bifurcation analysis shows that the loss of stability leads to a continuous transition from a critical system of identical drops to a stable system of axisymmetric non-identical drops. With increasing total protruded liquid volume this system of non-identical drops reaches its own collective stability limit (to axisymmetric perturbations) which gives rise to dripping or streaming from the holes. Critical volumes and heights for non-identical drops have been calculated as functions of the dimensionless hole radius (associated with the Bond number). For unequal hole radii, there are three intervals of the larger dimensionless hole radius, R_1^0, with qualitatively different bifurcation patterns which in turn can depend on the smaller dimensionless hole radius, R_2^0. Loss of stability may occur when the drop suspended from the larger hole reaches its stability limit (to non-axisymmetric perturbations) as a solitary drop or when the system reaches the collective stability limit (to axisymmetric perturbations). Typical situations are illustrated for selected values of R_1^0, and then the basic characteristics of the stability for a dense set of R_1^0 are presented.

1. Introduction

We consider an incompressible liquid region overlying a flat horizontal plate. Two pendant drops are pinned to the edges of two circular holes in the plate. The holes have radii r_1^0 and r_2^0 and are at the same hydrostatic level. The drops are connected by the liquid region. The total volume of liquid is constant. The liquid's free surface is assumed to consist only of the two axisymmetric drop surfaces, Γ_1 and Γ_2, and is, thus, a disconnected surface. The study of the stability of this system is a first and important step for the analysis of the stability of the system with a large number of holes with radii $r_1^0, \ldots, r_m^0$ and pendant drop surfaces $\Gamma_1, \ldots, \Gamma_m$ ($m > 2$). This is a typical geometry associated with, for example, devices such as perforated diaphragms and screens that underlie a liquid reservoir. These types of devices occur widely in the chemical, food and power industries. They are also of importance for space

applications such as propellant management systems created for localization and confinement of liquid at a designated location within a tank.

The stability of the systems with large numbers of holes may be roughly estimated from the results obtained in this study as follows: if the system of two drops is unstable, then any system that includes these two drops is also unstable. In addition to addressing the question of stability, we note that the accurate numerical data we obtain for critical parameter values for two drops suspended from equal radii holes provides a basis for an alternative method for surface tension measurement. Our results can also be used to guide design of 'electroosmotic droplet switches'. Vogel, Ehrhard & Steen (2005) discuss switches that take advantage of the existence of bi-stable droplet configurations for a given combined volume of two separate drops attached to equal radii holes when gravity is neglected. Our results could be used for switches with drops attached to unequal radii holes in weightlessness or to equal and unequal radii holes under axial gravity conditions (i.e. when the switch is gravity sensitive).

If an incompressible liquid volume is bounded by a disconnected free surface, it follows that any deformation of the liquid's surface must conserve the total liquid volume. For the case under consideration, the fixed volume condition takes the form

$$\delta v_1 + \delta v_2 = 0, \tag{1a}$$

or, equivalently,

$$\int_{\Gamma_1} N_1 \, \mathrm{d}\Gamma + \int_{\Gamma_2} N_2 \, \mathrm{d}\Gamma = 0. \tag{1b}$$

Here, δv_1 and δv_2 correspond to variations of the drop volumes v_1 and v_2, and N_i is the normal component of perturbations to the surface Γ_i $(i = 1, 2)$. However, the constant volume constraint (1a) does not require that each drop satisfy a separate volume conservation condition of the form

$$\delta v_1 = \delta v_2 = 0, \tag{2a}$$

or

$$\int_{\Gamma_1} N_1 \, \mathrm{d}\Gamma = \int_{\Gamma_2} N_2 \, \mathrm{d}\Gamma = 0. \tag{2b}$$

Isochoric perturbations that satisfy (2b) are precisely the disturbances that determine the stability of a solitary drop under a constant volume constraint (figure 1a). For the disconnected surface formed by the two connected drops considered here, the perturbation of a drop surface need not conserve the volume of that drop, but must be associated with a complementary non-isochoric perturbation of the other drop's surface such that the total liquid volume is conserved (see figure 1b). Consequently, the set of admissible perturbations on each drop surface Γ_1 and Γ_2 that must satisfy (1b) is larger than the set of isochoric perturbations that satisfy (2b). This means that collectively, two pendant drops may be more unstable than either of the two drops considered separately and with a constant volume constraint. This is the distinctive feature of systems with disconnected free surfaces (see, for example, Alexander & Slobozhanin 2004).

1.1. *The stability of a solitary pendant drop to isochoric perturbations*

The stability problem for two connected drops suspended from the edges of circular holes in a horizontal plate is closely related to the classical problem of solitary pendant

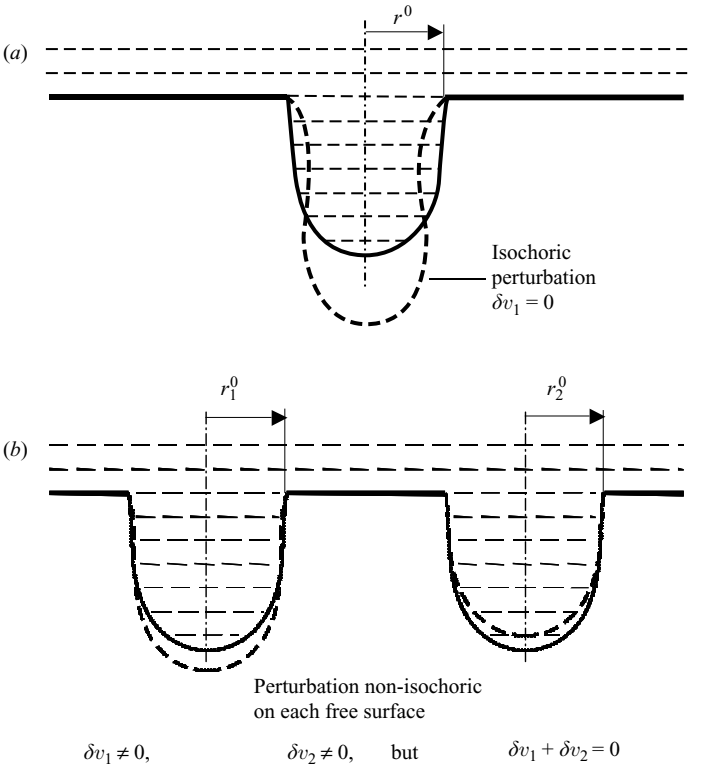

FIGURE 1. Equilibrium (thin solid lines) and perturbed (dashed lines) surfaces of pendant drops pinned to edges of holes in a horizontal plate (thick straight lines). (*a*) The perturbation is isochoric for a single drop. (*b*) The perturbation may be non-isochoric on each of the two connected drops.

drop stability. For solitary drops there are two cases – stability to constant-volume perturbations and stability to constant-pressure perturbations. Thompson (1979) and Michael (1981) refer to these as internal and external stability, respectively. For situations where the drop volume is constant, the admissible perturbations are isochoric. Previous results for drop stability to isochoric perturbations are summarized below.

In the absence of gravity, the equilibrium free surface of any axisymmetric drop pinned to the edges of circular holes is a spherical segment, has a minimal area and, thus, is always stable to small perturbations for which the surface remains pinned.

For gravity oriented perpendicular to a flat plate, the axisymmetric equilibrium shapes of pendant drop free surfaces pinned to edges in the plate have been thoroughly investigated both numerically and analytically (see Bashforth & Adams 1883; Freud & Harkins 1929; Concus 1968; Hida & Nakanishi 1970; Padday 1971; Boucher & Evans 1975; Vaček 1975; Hartland & Hartley 1976; Chesters 1977; Concus & Finn 1979; Finn 1986; Myshkis *et al.* 1987 and references therein). With $\sqrt{\sigma/\rho g}$ chosen as a characteristic length (ρ is the liquid density, g is the acceleration due to gravity, and σ is the surface tension) the equilibrium equations (described in § 2.1) can be normalized by a similarity transformation of cylindrical coordinates (r, θ, z) to non-dimensional variables (R, θ, Z). For a given dimensionless radius of the hole, R^0, there is a one-parameter family of axisymmetric equilibrium surfaces. The determining

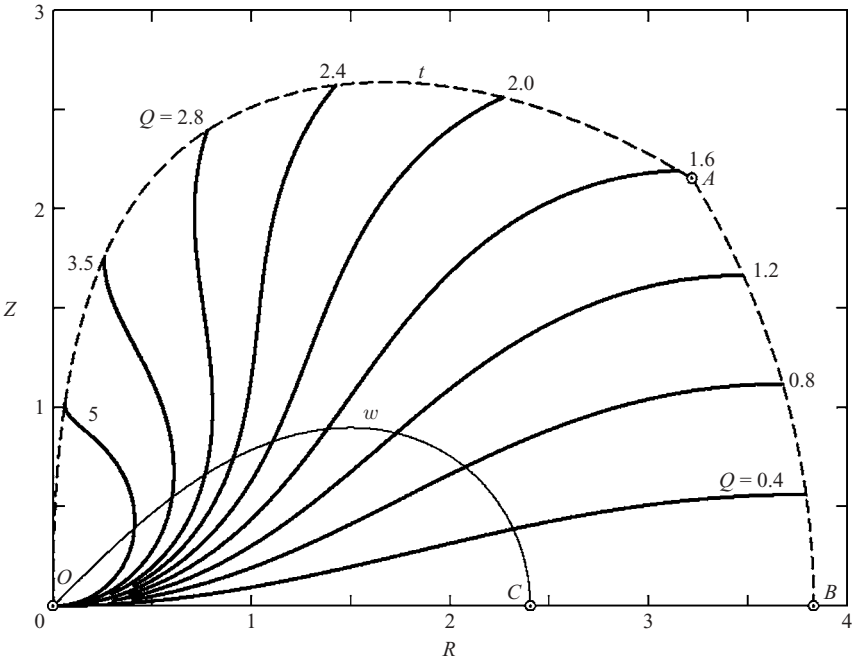

FIGURE 2. Profiles of single pendant drops critical to isochoric perturbations (thick solid lines). They are bounded by the dashed line $OtAB$. For $R^0 < 3.219$ (the terminal point of a critical profile lies on OtA), a drop loses its stability to axisymmetric perturbations. For $3.219 < R^0 < 3.8317$ (the terminal point belongs to AB) loss of stability occurs to non-axisymmetric perturbations (after Slobozhanin & Tyuptsov 1974; Myshkis *et al.* 1987). Drops with profiles bounded by the thin solid line OwC are critical to fixed pressure perturbations (after Slobozhanin & Alexander 2003). Lines $OtAB$ and OwC represent dependency of dimensionless height, H^*, on dimensionless hole radius, R^0, for solitary drops critical to isochoric perturbations and to fixed pressure perturbations, respectively.

parameter is twice the dimensionless mean curvature, Q, of a drop surface at the point of intersection with the Z-axis of symmetry. Segments of a set of equilibrium lines corresponding to axial sections $\theta = \text{const}$ of equilibrium free surfaces with coincident initial points (belonging to the Z-axis) are shown in figure 2. The gravity vector is downward-directed, and the liquid lies above the equilibrium surface. Only lines with $Q > 0$ are depicted. When Q changes sign, the equilibrium line undergoes a mirror reflection with respect to the R-axis (which coincides with the line $Q = 0$). Lines with $Q < 0$ correspond to sessile bubbles.

The internal stability of a solitary drop hanging from the edge of a hole was first analysed by Lonstein (1906*a–c*). He reasoned that a drop loses its stability when the drop volume takes a locally maximum value for a given radius of the hole, R^0. Freud & Harkins (1929) and later other authors (Padday & Pitt 1973; Boucher & Evans 1975; Pitts 1976; Vaček, Nekovář & Grigar 1977) used the Lonstein method to calculate stable drop shapes. A rigorous proof of the truth of the Lonstein method is due to Pitts (1974).

The Lonstein method holds only for the analysis of the stability to axisymmetric isochoric perturbations. However, they are not necessarily the most dangerous. Maxwell (1876) was the first to establish this. To explain the results of Duprez' experiment (1851, 1854), he analysed the stability of a horizontal free surface resting

on the edges of a hole and separating the liquid above from a gas below (a pendant 'drop' of a zero volume with equilibrium line $Q = 0$). He found that non-axisymmetric perturbations $Z = \varepsilon J_1(R)\cos\theta$ are the most dangerous (ε is a small amplitude), and that the critical radius R^0 is 3.8317 (corresponding to the first positive zero of the Bessel function $J_1(x)$). The stability of a drop with a curved free surface with respect to arbitrary perturbations (both axisymmetric and non-axisymmetric) was examined by Slobozhanin & Tyuptsov (1974, 1975) (see also Babskii *et al.* 1976; Myshkis *et al.* 1987, §§ 3.4.4, 3.9.5, 3.10). They have shown that a solitary drop loses stability to axisymmetric isochoric perturbations only for $R^0 < 3.219$. However, if $3.219 < R^0 < 3.8317$, non-axisymmetric perturbations $N = \varepsilon Z'(S)\cos\theta$ become more dangerous (S is the dimensionless arclength of an equilibrium line), and no stable state exists for $R^0 > 3.8317$. On the interval $3.219 < R^0 < 3.8317$ the profiles (axial sections) of critical drops correspond to $0 < Q < 1.570$ and have horizontal tangents at their endpoints $S = S_1^*$. Segments of equilibrium lines depicted in figure 2 represent profiles of drops critical to arbitrary perturbations. The dependence of their height $H^* = Z(S_1^*;\, Q)$ and protruded volume

$$V^* = \pi \int_0^{S_1^*} R^2(S;\, Q)\, Z'(S;\, Q)\, \mathrm{d}S$$

on R^0 has been constructed (see figures 2 and 3). It should be emphasized that non-axisymmetric perturbations are always isochoric (in contrast to axisymmetric perturbations that may be either isochoric or non-isochoric).

Michael & Williams (1976) independently drew the same conclusion, i.e. that non-axisymmetric perturbations are critical for $3.219 < R^0 < 3.8317$. A discussion of solitary pendant drop stability is available in a review by Michael (1981). Many of the mathematical aspects of pendant drop stability were studied by Wente (1980, 1989).

Bifurcation patterns described by Myshkis *et al.* (1987, § 4.4.2) lead to the conclusion that loss of stability of an axisymmetric pendant drop, either to axisymmetric isochoric perturbations or to non-axisymmetric perturbations, results in the liquid dripping or streaming out from the hole.

The results of previous investigations of pendant drop stability to isochoric perturbations have typically been presented graphically. Figures collected in tables (Freud & Harkins 1929; Boucher & Evans 1975; Myshkis *et al.* 1987) are not sufficiently detailed and accurate for practical use. In addition, the characteristics of critical drops are given as functions of Q, a value that cannot be predetermined and is difficult to measure. However, the detailed numerical data are of immediate interest to the experimentalist, and in the context of the present study, are necessary for at least two reasons: (*a*) to have the opportunity to compare accurately the stability of a solitary drop and two connected drops hanging from holes of equal radii; and (*b*) for the case of two drops hanging from holes with unequal radii, to calculate the parameters of the critical system determined by the drop hanging from the larger hole and critical to non-axisymmetric perturbations (see § 5). We have performed accurate calculations with an integration step in the dimensionless arclength S equal to 10^{-6} and a dimensionless radius R^0 determined to within 10^{-5}. These calculations yielded data for the critical parameters H^*, V^*, Q^*, $Q^* - H^*$, and the slope angle $\beta^* = \beta(S_1^*; Q^*)$ at the endpoints of critical profiles. These parameters were determined for a dense set of R^0 values with an increment 0.05 and can be requested directly from the authors.

1.2. *Relation between the stability of a solitary drop to fixed-pressure perturbations and the stability of connected drops to fixed-volume perturbations*

Alexander & Slobozhanin (2004) reviewed methods suggested by Gillette & Dyson (1974), Orel (1974), Maddocks (1987) and Lowry & Steen (1995) to examine the stability of systems with multiple free surfaces. Orel (1974) must be given credit for first recognizing the importance of fixed-pressure stability of single surface systems to the stability of fixed liquid volumes with coupled free surfaces. Slobozhanin & Alexander (2003) have shown that:

(i) A system of m, $m \geqslant 2$, connected drops is stable to perturbations which conserve the total liquid volume (see condition (1a) for the case $m = 2$) if, when considered separately as a solitary pendant drop, each of the drops that comprise the system is stable to constant-pressure perturbations.

(ii) The system is unstable if, when considered separately as a solitary pendant drop, at least two of the drops that comprise the system are unstable to constant-pressure perturbations.

In this connection the stability conditions under fixed-pressure perturbations (or external stability) for a solitary drop hanging from the edges of a hole are important.

Under zero-gravity, a free surface is the surface of a spherical segment. A solitary spherical segment is stable to fixed-pressure perturbations if it is less than a hemisphere, and is unstable if it is greater than a hemisphere (Boys 1902; Searle 1934). (This is in contrast to fixed-volume perturbations for which any spherical segment pinned to edges is stable.)

For non-zero gravity, Pitts (1974) has calculated the critical volume, V^*, of a solitary pendant drop under constant-pressure perturbations for $R^0 = 1$ and 2, and Michael & Williams (1976) have constructed a set of curves that permit calculation of the critical height H^* for selected values of R^0 on the interval $0.6 \leqslant R^0 \leqslant 2.0$. A solitary 'drop' with a horizontal free surface is stable if $R^0 < 2.4048$ (this is the value of the first zero of the Bessel function $J_0(x)$). This condition was obtained by Pitts (1974) and Michael & Williams (1976). For $R^0 > 2.4048$, there is no solitary drop stable to fixed-pressure perturbations. Under a fixed pressure constraint, axisymmetric perturbations are always the most dangerous. The comprehensive calculations related to this kind of stability were performed by Slobozhanin & Alexander (2003), and the functions $H^*(R^0)$ and $V^*(R^0)$ were constructed on the interval $0 < R^0 \leqslant 2.4048$ (see figures 2 and 3). Comparison of the stability regions for a solitary drop under perturbations constrained by either fixed pressure or fixed volume shows that these regions differ considerably in extent. For example, the maximum value of the critical height, H^*, is 2.638 for fixed-volume perturbations (this value corresponds to a solitary drop with $Q = 2.275$ that is suspended from a circular hole of radius $R^0 = 1.675$), and is 0.897($Q = 1.454$, $R^0 = 1.499$) for fixed-pressure perturbations (figure 2). As indicated in figure 3, the maximum dimensionless protruded liquid volume that can be retained under constant-volume perturbations is 18.964 (the critical solitary drop corresponding to $Q = 1.570$ and $R^0 = 3.219$). In contrast, for fixed-pressure perturbations, this volume is 4.379 ($Q = 0.900$ and $R^0 = 1.995$). Detailed numerical information about parameters of drops critical to fixed-pressure perturbations can also be requested from the authors. The presented values have high accuracy (as in the case of solitary drops critical to isochoric perturbations).

According to the conclusions (i) and (ii), stated above, a system consisting of two pendant drops is stable to perturbations that conserve total volume if the profiles of both downwardly protruding drops belong to the region $OwCO$ in figure 2. The system is unstable if the terminal points of both profiles lie outside this region (as a

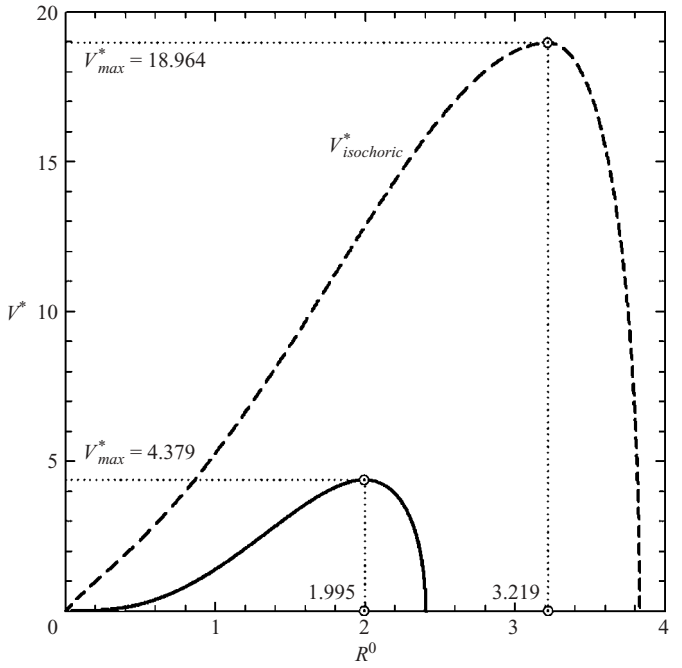

FIGURE 3. Dimensionless volume as a function of R^0 for a single pendant drop critical to isochoric perturbations (dashed line; after Slobozhanin & Tyuptsov 1975 and Myshkis *et al.* 1987) and to fixed pressure perturbations (solid line; Slobozhanin & Alexander 2003).

clear example, if dimensionless holes radii $R_1^0 > 2.4048$ and $R_2^0 > 2.4048$). In particular, if $R_1^0 = R_2^0$ and the profiles of the two drops are identical, the system stability is the same as the stability of a solitary drop suspended from the edges of a horizontal circular hole and subject to constant-pressure perturbations.

Note, however, that even for equal holes ($R_1^0 = R_2^0$), two drops are not necessarily identical. The general case that remains unsolved is the case when one drop (when considered as a solitary drop) is stable to fixed-pressure perturbations while the other is unstable to these perturbations but is stable to isochoric perturbations, (2*b*). In other words, this is the case when the terminal point of one equilibrium profile belongs to the region $OwCO$, while the terminal point of other profile lies in the region $OtABCwO$ (figure 2). Only these systems may be critical for connected non-identical drops and non-isochoric perturbations, (1*b*).

In the following, for clarity, we refer to IC-perturbations as the perturbations that conserve the volume of each of two connected drops independently (i.e. they satisfy the condition (2*b*)). On the other hand, we refer to NI-perturbations as the perturbations that do not conserve the volume of either of the two drops independently (i.e. they satisfy the condition (1*b*), but do not satisfy the condition (2*b*)). A solitary drop that is stable (unstable) to isochoric perturbations is IC-stable (IC-unstable). A solitary drop that is stable (unstable) to constant-pressure perturbations is CP-stable (CP-unstable). It is evident that a system of two connected drops must be unstable (to IC-perturbations) if at least one of the drops is IC-unstable. However, this does not always determine the stability limit of a system of two drops. As discussed earlier, in some cases, the range of stable two-drop configurations may be smaller than would be predicted by a consideration of solitary drop stability to IC-perturbations because the

drops may lose stability to NI-perturbations. A system of two connected drops that is stable (unstable) to NI-perturbations is NI-stable (NI-unstable). Consistent with this nomenclature we refer to critical states as IC-critical, CP-critical or NI-critical.

The organization of this paper is as follows. In § 2, we outline previous approaches to the study of the equilibrium and stability conditions of two connected pendant axisymmetric drops. The case of zero-gravity (§ 3) is relatively simple, and the stability conditions for a weightless liquid bounded by two spherical segments in contact with the edges of equal radii holes are known. In this paper, we examine the effect of unequal hole radii. For two pendant drops under non-zero gravity, we first focus attention on equal radii holes (§ 4). Our results are illustrated in detail using the example of $R_1^0 = R_2^0 = 1$. Then for the case of arbitrary $R_1^0 = R_2^0$ values, the parameters determining the critical states are presented. For systems with unequal radii holes, $R_1^0 > R_2^0$, we proceed from the simplest case when a liquid is bounded from below by horizontal free surfaces pinned to edges of two holes in a horizontal plate. We then deal with curved free surfaces, and present results for three intervals of the larger hole radius, R_1^0, where we found quite different stability and bifurcation behaviour (§ 5). Within each of these intervals a representative value of R_1^0 was chosen, the stability limit parameters were calculated and illustrated as functions of R_2^0. To verify the repeatability of these distinctive features of the stability patterns within each interval, the same calculations were performed for other selected values of R_1^0.

2. Formulation of the problem

2.1. *The equilibrium surface problem*

We introduce cylindrical coordinates (r_i, θ_i, z_i) in the neighbourhood of each of the axisymmetric equilibrium surfaces $\Gamma_i (i = 1, 2)$ and place the origin at the tip of Γ_i. Then a parametric representation $r_i = r_i(s_i)$, $z_i = z_i(s_i)$ of the surface Γ_i (s_i is the arclength of an axial section $\theta_i = \text{const}$ of Γ_i) is the solution to (Myshkis *et al.* 1987)

$$r_i'' = -z_i' \beta_i', \quad z_i'' = r_i' \beta_i', \quad \beta_i' = -b z_i + q_i - z_i'/r_i \quad (0 \leqslant s_i \leqslant s_{i1}, \ ' = \mathrm{d}/\mathrm{d}s_i), \tag{3}$$

$$r_i(0) = z_i(0) = z_i'(0) = 0, \quad r_i'(0) = 1, \quad \beta_i(0) = 0. \tag{4}$$

The section $\theta_i = \text{const}$ determinates the profile of the surface Γ_i; $\beta_i(s_i)$ is the angle between the r_i-axis direction and the tangent to the equilibrium profile which is directed in the sense of increasing s_i; $\beta_i'(s_i)$ is the curvature of the profile; $b = \rho g/\sigma$ is the capillary constant; $s_i = 0$ and $s_i = s_{i1}$ are the profile's initial and terminal points; q_i is twice the mean curvature of the surface Γ_i at the point $s_i = 0$. System (3) represents the Gauss–Laplace capillary equation. The terminal points $s_i = s_{i1}$ of the equilibrium profiles must satisfy the conditions

$$r_i(s_{i1}; q_i) = r_i^0 \quad (i = 1, 2), \tag{5}$$

where r_i^0 are the hole radii, while the parameters q_1 and q_2 are related by the condition that the liquid pressures are equal where the drop surfaces meet the plate

$$q_1 - b z_1(s_{11}; q_1) = q_2 - b z_2(s_{21}; q_2). \tag{6}$$

The volume v_i of each drop is

$$v_i = \pi \int_0^{s_{i1}} r_i^2(s_i; q_i) z_i'(s_i; q_i) \, \mathrm{d}s_i. \tag{7}$$

2.2. *The stability problem*

The determination of stability is based on an analysis of the second variation of the potential energy under arbitrary perturbations subject to the constant volume constraint, (1*a*). The mathematical approach follows the method described in Slobozhanin (1983) and Myshkis *et al.* (1987, § 3.12).

(*a*) *Stability to axisymmetric perturbations that are non-isochoric on each* Γ_i

Arbitrary perturbations can be represented in the form

$$N_i(s_i,\ \theta_i) = \varphi_i(s_i) + \sum_{n=1}^{\infty} [\varphi_{in}(s_i)\cos(n\theta_i) + \psi_{in}(s_i)\sin(n\theta_i)]. \tag{8}$$

Since non-axisymmetric perturbations ($n \geqslant 1$) are isochoric, only axisymmetric perturbations need be analysed in the study of the stability to NI-perturbations on each surface Γ_i.

This stability problem is reduced to the determination of the sign of the smallest eigenvalue λ_1 of the following boundary problem:

$$L_i\varphi_i + \mu = \lambda\varphi_i \quad (0 \leqslant s_i \leqslant s_{i1};\quad i = 1, 2), \tag{9}$$

$$\varphi_i(s_{i1}) = 0, \qquad \sum_{i=1}^{2} \int_0^{s_{i1}} r_i\,\varphi_i\,\mathrm{d}s_i = 0, \tag{10a, b}$$

where

$$L_i\varphi_i \equiv -\varphi_i'' - \frac{r_i'}{r_i}\,\varphi_i' + [-br_i' - (z_i'/r_i)^2 - \beta_i'^2(s_i)]\,\varphi_i. \tag{11}$$

The equilibrium is stable if $\lambda_1 > 0$, and is unstable if $\lambda_1 < 0$. An unknown constant μ is determined from the condition (10*b*). This condition means that all perturbations adhere to the condition (1*b*). It should be emphasized that the problem (9)–(10) involves both surfaces Γ_1 and Γ_2 and cannot be split into two independent problems for each Γ_i. It can be deduced from results presented in Slobozhanin (1983) and Myshkis *et al.* (1987) that the stability condition ($\lambda_1 > 0$) assumes the form

$$u_1(s_{11})\,D_2(s_{21}) + u_2(s_{21})\,D_1(s_{11}) < 0. \tag{12}$$

Here,

$$D_i(s_i) = u_i(s_i)\int_0^{s_i} r_i(s_i)\,f_i(s_i)\,\mathrm{d}s_i - f_i(s_i)\int_0^{s_i} r_i(s_i)u_i(s_i)\,\mathrm{d}s_i, \tag{13}$$

$u_i(s_i)$ and $f_i(s_i)$ are the solutions (bounded at $s_i = 0$) of the equations

$$L_i u_i = 0, \qquad L_i f_i + 1 = 0. \tag{14}$$

(*b*) *Stability to perturbations that are isochoric on each* Γ_i

To examine the stability to IC-perturbations we use the method described by Myshkis *et al.* (1987, §§ 3.3, 3.9). For a given q_i, the surface Γ_i is stable to axisymmetric IC-perturbations if the terminal point $s_{i1} < s_{i1}^*$, is critical if $s_{i1} = s_{i1}^*$, and is unstable to these perturbations if $s_{i1} > s_{i1}^*$. Here, $s_i = s_{i1}^*$ is the first zero of the function $D_i(s_i)$.

The surface Γ_i is critical to non-axisymmetric perturbations if

$$z_i'(s_{i1}) = 0 \tag{15}$$

and $z_i'(s_i) \neq 0$ on the interval $0 < s_i < s_{i1}$.

3. Zero gravity

3.1. *Stability condition*

Under zero-gravity conditions ($b=0$), the equilibrium surface consists of two spherical segments of equal radii, $\wp_1=\wp_2\equiv\wp_0$, so that $q_1=q_2\equiv q_0$. The shapes and characteristics are described as

$$r_i=\frac{2}{q_0}\sin\frac{q_0 s_i}{2},\quad z_i=\frac{2}{q_0}\left(1-\cos\frac{q_0 s_i}{2}\right),\quad \beta_i=\tfrac{1}{2}q_0 s_i, \tag{16}$$

$$v_i=\frac{8\pi}{3q_0^3}\left(1-\cos\frac{q_0 s_{i1}}{2}\right)^2\left(2+\cos\frac{q_0 s_{i1}}{2}\right). \tag{17}$$

Since

$$u_i=\cos\frac{q_0 s_i}{2},\quad f_i=\frac{2}{q_0^2},\quad D_i(s_i)=-\frac{4}{q_0^4}\left(1-\cos\frac{q_0 s_i}{2}\right)^2, \tag{18}$$

the stability condition (12) can be written in the form

$$\cos\beta_{11}(1-\cos\beta_{21})^2+\cos\beta_{21}(1-\cos\beta_{11})^2>0, \tag{19}$$

where $\beta_{i1}=q_0 s_{i1}/2$ is the polar angle of the spherical segment Γ_i.

3.2. *Equal radii holes*

It follows from (5) and (16) that for holes of equal radii ($r_1^0=r_2^0\equiv r^0$) we have either $\beta_{11}=\beta_{21}$ or $\beta_{11}+\beta_{21}=180^\circ$. According to (19), a pair of identical segments ($\beta_{11}=\beta_{21}$) is stable if $\beta_{11}=\beta_{21}<90^\circ$, and is unstable if $\beta_{11}=\beta_{21}>90^\circ$. (This is in agreement with result of Searle, 1934, that the stability limit for a solitary spherical segment perturbed under a constant-pressure constraint is a hemisphere and with the statements (i) and (ii) in § 1.2.) It also follows from (19) that non-identical segments ($\beta_{11}\neq\beta_{21}$, $\beta_{11}+\beta_{21}=180^\circ$) are stable.

The above results are well known. They were explained by Boys (1902) more than 100 years ago. As the total protruded volume of two drops exceeds that for two hemispheres, the stable system consists of two non-identical drops. This is because the segments Γ_1 and Γ_2 with $\beta_{11}+\beta_{21}=180^\circ$ are the complements to an entire sphere, and their total area assumes a global minimum for a given total volume. The critical state of two hemispheres is stable for the same reason. Thus, loss of stability of a pair of identical spherical segments results in a continuous transition to a stable system of non-identical segments. This was also described later by Adamson (1960).

The stability of segments pinned to edges of equal radii holes has been clearly demonstrated by the bifurcation diagram drawn by Wente (1999) and shown in figure 4. Here, the relative volumes, $\bar V_1$ and $\bar V_2$, and the total relative volume, $\bar V_{tot}$, are determined as

$$\bar V_i=v_i/[\pi(r^0)^3]\quad(i=1,2),\qquad \bar V_{tot}=\bar V_1+\bar V_2. \tag{20}$$

The bifurcation point $\bar V_{tot}=4/3$ corresponds to two hemispheres. For $\bar V_{tot}>4/3$, there exist three equilibrium states: an unstable state with two identical spherical caps greater than a hemisphere ($\beta_{11}=\beta_{21}>90^\circ$), and two stable states with unequal spherical caps. On the upper branch ($\bar V_1-\bar V_2>0$), the first cap is greater than a hemisphere ($\beta_{11}>90^\circ$), and the second is less than a hemisphere ($\beta_{21}<90^\circ$). In contrast, the lower branch ($\bar V_1-\bar V_2<0$) corresponds to states with $\beta_{11}<90^\circ$ and $\beta_{21}>90^\circ$. Clearly, these branches are symmetric about the horizontal line $\bar V_1-\bar V_2=0$. It should be stressed that loss of stability of identical spherical caps occurs with respect to NI-perturbations.

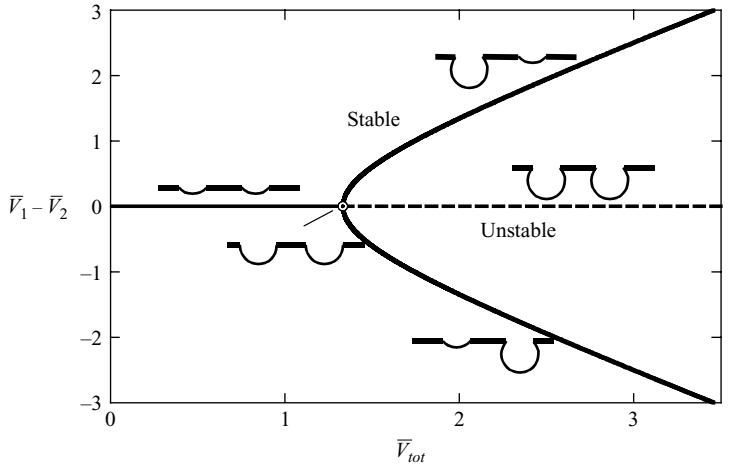

FIGURE 4. Bifurcation diagram for the system of two zero-gravity drops in contact with edges of equal radii holes (after Wente 1999). Solid (dashed) lines correspond to stable (unstable) states. Inserts depict characteristic shapes of the states. The open circle ($\bar{V}_{tot} = 4/3$, $\bar{V}_1 - \bar{V}_2 = 0$) corresponds to the state with two hemispheres.

3.3. *Unequal radii holes*

Hereinafter, in studies of the stability problem for unequal holes we assume that $r_1^0 > r_2^0$. Then,

$$K \equiv r_2^0 / r_1^0 \leqslant 1. \tag{21}$$

In definition of the relative volumes, the radius r_1^0 is used as characteristic length, so that instead of (20) we have

$$\bar{V}_i = v_i / \left[\pi \left(r_1^0\right)^3\right] \qquad (i = 1, 2). \tag{22}$$

The volumes $\bar{V}_{tot}$ and $\bar{V}_1 - \bar{V}_2$ can be presented in the form

$$\bar{V}_{tot} = \frac{1}{3 \sin^3 \beta_{11}} [(1 - \cos \beta_{11})^2 (2 + \cos \beta_{11}) + (1 - \cos \beta_{21})^2 (2 + \cos \beta_{21})], \tag{23}$$

$$\bar{V}_1 - \bar{V}_2 = \frac{1}{3 \sin^3 \beta_{11}} [(1 - \cos \beta_{11})^2 (2 + \cos \beta_{11}) - (1 - \cos \beta_{21})^2 (2 + \cos \beta_{21})], \tag{24}$$

where β_{11} and β_{21} are related by

$$\sin \beta_{21} = K \sin \beta_{11}. \tag{25}$$

For a given K ($0 < K < 1$), a typical bifurcation diagram is shown in figure 5. It consists of isolated solutions that perturb a classical pitchfork bifurcation for $K = 1$. Such behaviour is well-known (see, for example, Iooss & Joseph 1997, chap. 3). The left-hand segment, OA, of the upper branch corresponds to a system of two spherical caps less than a hemisphere ($\beta_{11} < 90°$, $\beta_{21} < 90°$). Clearly, these states are stable (since each cap is CP-stable). Branch Ak represents states with the first cap greater ($\beta_{11} > 90°$) and the second cap smaller ($\beta_{21} < 90°$) than a hemisphere. Calculations have shown that the stability condition (19) holds for all these states and any $K, 0 < K < 1$. The branch Bm represents systems for which both spherical caps are greater than a hemisphere ($\beta_{11} > 90°$, $\beta_{21} > 90°$). These systems are NI-unstable. If the first cap is smaller ($\beta_{11} < 90°$) and the second is greater than a hemisphere, the

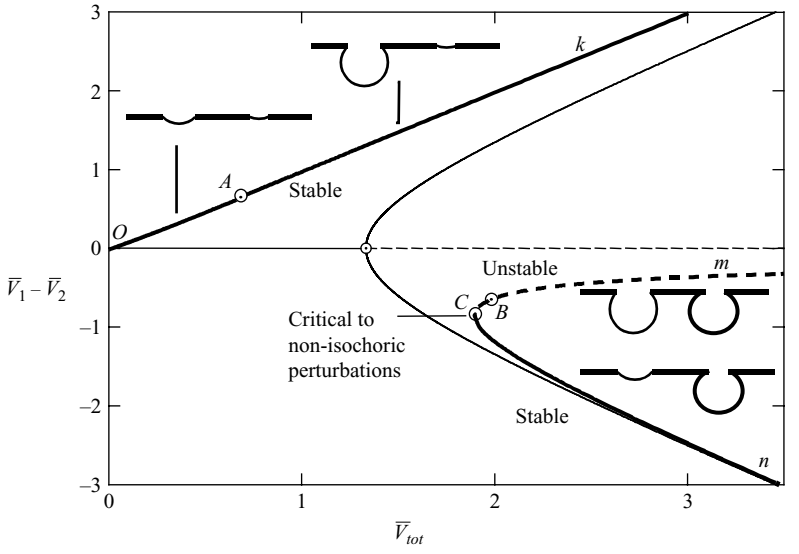

FIGURE 5. Bifurcation diagram for the system of two zero-gravity drops in contact with edges of unequal radii holes ($K = 0.5$). Solid and dashed lines correspond to stable and unstable states, respectively. Thin lines relate to the case of $K = 1$ (see figure 4). Inserts show configurations of equilibrium states.

	R^0			
K	β_{11}	β_{21}	$\bar{V}_{tot}$	$\bar{V}_1 - \bar{V}_2$
0.1	80.12°	174.35°	1.914	−0.875
0.2	80.12°	168.64°	1.914	−0.875
0.3	80.12°	162.81°	1.912	−0.873
0.4	80.13°	156.79°	1.907	−0.868
0.5	80.15°	150.49°	1.897	−0.857
0.6	80.20°	143.75°	1.877	−0.836
0.7	80.30°	136.37°	1.842	−0.798
0.8	80.53°	127.90°	1.779	−0.729
0.9	81.14°	117.22°	1.665	−0.600

TABLE 1. Characteristics of NI-critical zero-gravity systems consisting of two spherical drops in contact with edges of unequal radii holes for different values of $K \equiv r_2^0/r_1^0$.

system may be stable or unstable. The segment BC and the branch Cn (figure 5) represent unstable and stable states, respectively, while the critical state corresponds to the point C which is a regular turning point. Characteristics of the critical systems for a set of K are given in table 1. The values of β_{11} for stable states are less than the critical value.

4. Effect of gravity: drops hanging from equal radii holes

For non-zero gravity ($b \neq 0$), we use $b^{-1/2}(\equiv \sqrt{\sigma/\rho g})$ as the characteristic length and employ the following dimensionless variables and values

$$R_i = \sqrt{b}\, r_i, \quad Z_i = \sqrt{b}\, z_i, \quad S_i = \sqrt{b}\, s_i, \quad Q_i = q_i/\sqrt{b}, \quad V_i = b^{3/2}\, v_i. \tag{26}$$

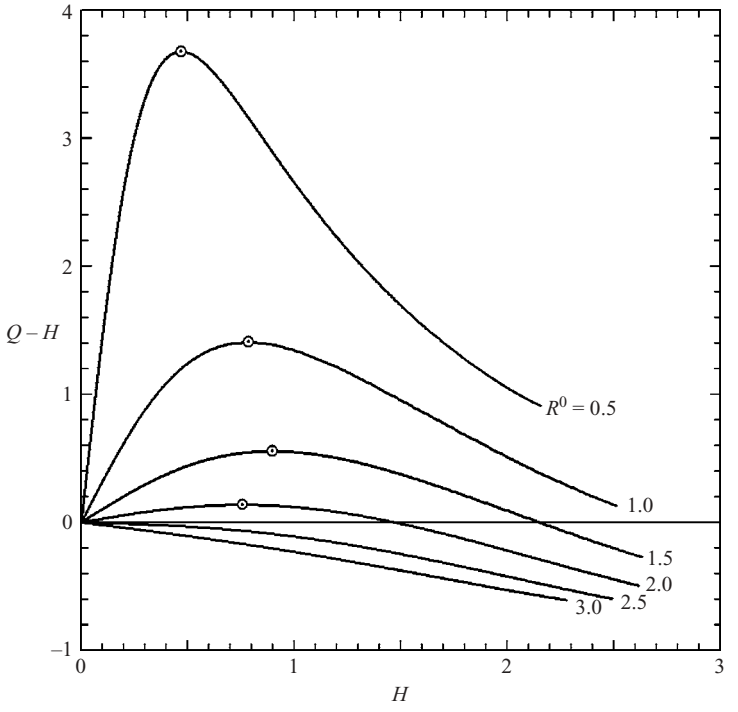

FIGURE 6. Dimensionless pressure difference across the interface in the plane of hole, $Q-H$, for different dimensionless values R^0 of the hole radius as a function of dimensionless drop height, H.

Under this transformation, we should set $b=1$ in equations (3), (6) and (11). When dealing with characteristics that are the same for both drops, the sub index i ($i=1, 2$) will be omitted.

4.1. *Reference pressure characteristics*

When two separate equilibrium drops pinned to the edges of holes are linked, they form an equilibrium system only when

$$Q_1 - H_1 = Q_2 - H_2, \tag{27}$$

where H_i is the dimensionless height of the ith drop. This relationship for two connected equilibrium drops follows from the constraint (6). Hence, the variation of $(Q-H)$ along the vertical line $R=R^0$ (figure 2) corresponding to a given hole radius is one of the most important characteristics of pendant drops.

For selected values of R^0, the function $(Q-H)$ of H is shown in figure 6. The initial point (the origin) corresponds to a 'drop' with horizontal free surface ($Q=0,\ H=0$), while the terminal point of each line corresponds to the solitary drop which is IC-critical (i.e. to the drop with the profile bounded in figure 2 by the point of intersection of the vertical line $R=R^0$ and the boundary $OtAB$). The distinctive feature of each curve related to $R^0<2.4048$ is that it has a point with a maximum value of $(Q-H)$. This point exactly corresponds to the solitary drop that is CP-critical (i.e. to the drop with the profile bounded in figure 2 by the point of intersection of the vertical line $R=R^0$ and the curve OwC). To the left of this point, drops on the curve are CP-stable while to the right they are CP-unstable. The maximum $(Q-H)$ tends to

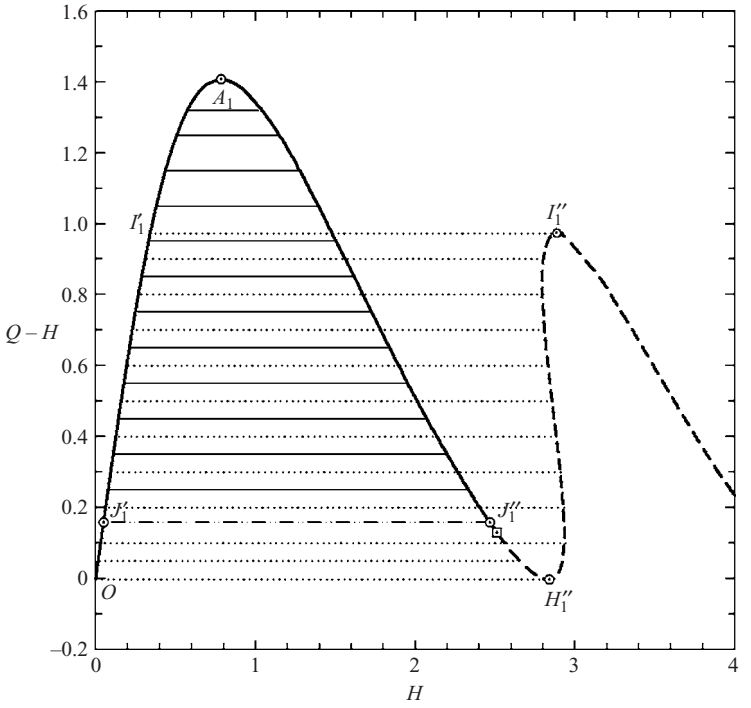

FIGURE 7. $Q-H$ for drops hanging from holes of equal radii, $R_1^0 = R_2^0 = 1$. Two connected identical drops are stable if the point lies on OA_1, and are unstable otherwise. Horizontal thin solid lines (dotted lines) depict a correspondence between two non-identical stable (unstable) drops. Two non-identical drops with respective points J_1' and J_1'' form a critical system. A single drop corresponding to the dot-square point is critical to isochoric perturbations. Branch I, OA_1-identical; branch II–1, A_1J_1'–A_1J_1''; branch II–2, OI_1'–$J_1''H_1''I_1''$; branch III ($A_1''H_1''I_1''$-identical).

the origin as $R^0 \to 2.4048$. The maximum value of $(Q-H)$ as a function of R^0 can be found in Slobozhanin & Alexander (2003). Points of curves with $R^0 > 2.4048$ (figure 6) correspond to CP-unstable solitary drops. The value of $(Q-H)$ along these curves decreases monotonically and is negative everywhere except the origin.

4.2. *The case* $R_1^0 = R_2^0 = 1$

To illustrate the stability of two connected drops with free surfaces pinned to edges of equal radii holes, we first consider the case of $R_1^0 = R_2^0 = 1$. A family of equilibrium drops exists along the curve shown in figure 7. Any solitary drop along the segment OA_1 is CP-stable. To the right of point A_1, solitary drops are CP-unstable. If two connected drops are represented by the same point on the segment OA_1 in figure 7, the drops are identical and according to conclusion (i), stated in § 1.2, form a stable system. Stable systems of identical drops correspond to points of branch I in the bifurcation diagram (figure 8). This branch is a horizontal segment $V_1 - V_2 = 0$, $0 \leqslant V_{tot} \leqslant 2.798$. As volume $V_{tot} \equiv V_1 + V_2$ increases from 0 to 2.798, a continuous shape evolution occurs for identical drops. The terminal point of each profile moves along the vertical line $R = 1$ from $Z = 0$ up to a point on the curve OwC. The terminal point on this curve determines the critical profile for connected identical drops.

If two drops are represented as a point to the right of point A_1 (figure 7), they correspond to an unstable system of connected identical drops. Such a system

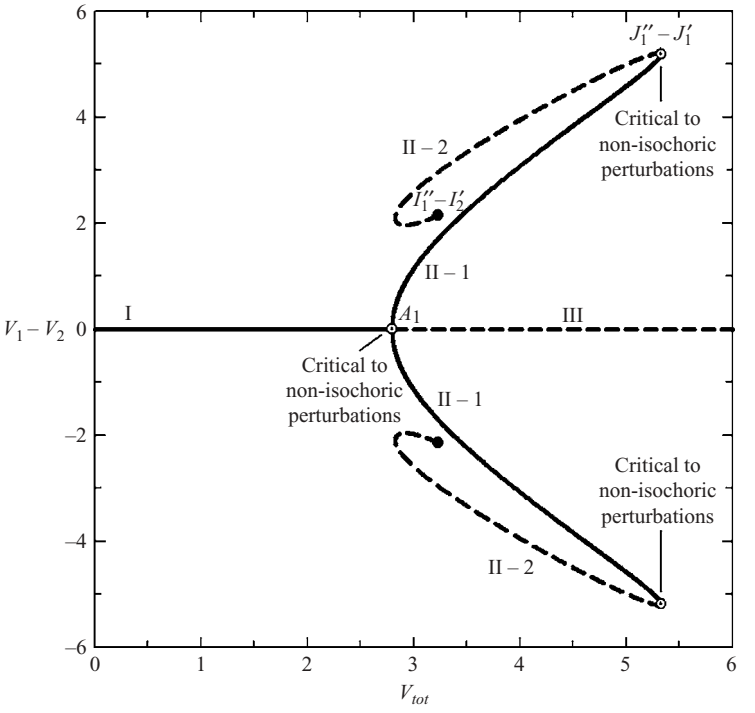

FIGURE 8. Bifurcation diagram for the system of two drops hanging from holes of equal dimensionless radii, $R_1^0 = R_2^0 = 1$. Solid (dashed) lines correspond to stable (unstable) systems.

corresponds to a point on branch III (figure 8), and the terminal point of the profile lies on the line $R = 1$ above the curve OwC.

Two non-identical drops are in equilibrium if they have equal values of $(Q - H)$. A correspondence between these drops is established through the horizontal tie-lines shown in figure 7. The most interesting is the case when one drop is CP-stable and the other drop is CP-unstable. According to our calculations, states of pairs of non-identical drops that bifurcate from the limiting pair of stable identical drops are stable. In other words, a system of two connected drops [with equal $(Q - H)$] that corresponds to two points that lie in the neighbourhood of the point A_1 (figure 7) is stable. The stability holds as the $(Q - H)$ value decreases until the critical state determined by the points J_1' and J_1'' is attained. It should be emphasized that here the system loses stability to NI-perturbations, and this occurs slightly earlier than for a solitary drop that is critical to IC-perturbations (see the adjacent point marked by a square).

On the bifurcation diagram, the branch labelled as II – 1 (figure 8) relates to stable non-identical drops. As the total protruded volume, V_{tot}, increases and passes through 2.798, a continuous transition (pitchfork bifurcation) occurs from a critical system of identical drops to a stable system of non-identical drops. The system of two non-identical drops remains stable until the total protruded volume reaches the local maximum value of 5.330. The critical state $J_1' - J_1''$ corresponds to this maximum value and is a turning point. The branch II – 2 relates to unstable systems of connected non-identical drops. One of these drops is CP-unstable and corresponds to a point on the segment $J_1'' H_1'' I_1''$ (figure 7) and the other is CP-stable (the correspondence between the drops is shown by dotted lines). The endpoint I_1'' in this correspondence

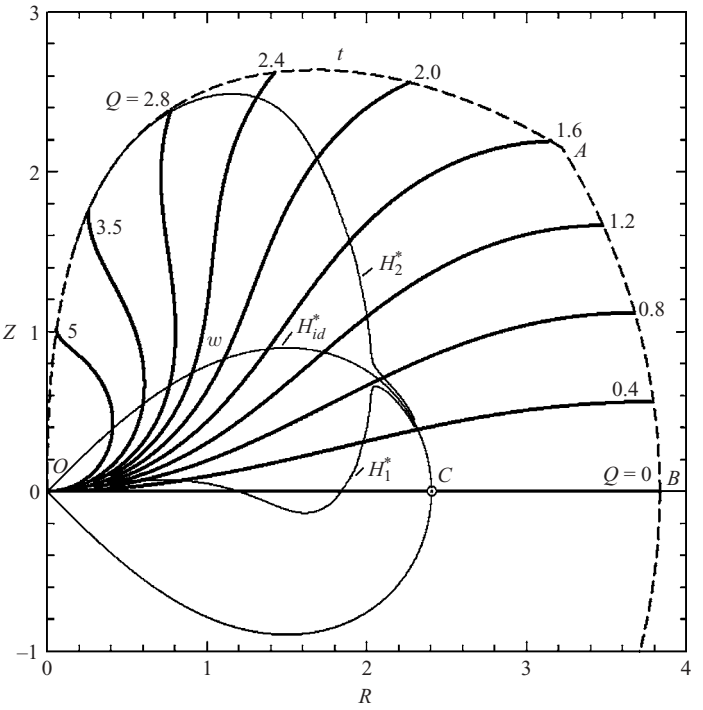

FIGURE 9. Dimensionless heights, H_1^* and H_2^*, of critical non-identical drops suspended from equal radii holes in comparison with dimensionless height, H_{id}^*, of identical critical drops (thin solid lines). These lines determine the terminal points for profiles of related critical drops.

was chosen arbitrarily. For example, such a correspondence may be extended beyond the point I_1'' to higher values of H, but it will not lead to a change in the stability.

For total volumes that exceed the critical value 2.798 for identical drops, the stable system consists of two non-identical drops. One of them has a volume greater than the critical volume of 1.399 and is CP-unstable. In contrast, the volume of the other drop is less than 1.399, and this drop is CP-stable. The deviation of each drop from the shape of critical identical drops increases with V_{tot}. A critical system of non-identical drops is determined by two drops with $V_{tot} = 5.330$. Upon further increase in V_{tot}, the system loses its stability, and the liquid is expected to drip or stream from the holes.

In contrast to the zero-gravity case, it can be seen that connected non-identical pendant drops reach their stability limit as the total dimensionless protruded liquid volume increases.

4.3. *The general case*

In a qualitative sense, the stability features described above for $R_1^0 = R_2^0 = 1$ are common to all equal radii holes $R_1^0 = R_2^0 = R^0$ with $0 < R^0 < 2.4048$. As discussed earlier, the line OwC in figure 2 represents the hole radius $R = R^0$ dependence of the critical height for identical drops, $Z = H_{id}^*$. For connected identical drops, the critical volume of each drop as a function of R^0 is shown in figure 3 by the solid line.

To find the critical systems for pairs of non-identical drops, calculations were carried out for a set of R^0 values with increments in the range from 0.01 to 0.05 (see table 2). The shape of critical drops can be estimated from figure 9, where the curves H_1^* and H_2^* are presented along with the curve H_{id}^* and the typical equilibrium profiles. The

R^0	H_1^*	V_1^*	Q_1^*	H_2^*	V_2^*	Q_2^*	$(Q-H)^*$
0.0500	0.0027	0.0000	4.2484	0.9624	0.2808	5.2082	4.2457
0.1000	0.0078	0.0001	3.1002	1.2520	0.5312	4.3444	3.0924
0.1500	0.0142	0.0005	2.5022	1.4557	0.7665	3.9437	2.4880
0.2000	0.0212	0.0013	2.1054	1.6141	0.9943	3.6983	2.0842
0.2500	0.0286	0.0028	1.8122	1.7429	1.2191	3.5266	1.7836
0.3000	0.0359	0.0051	1.5817	1.8507	1.4443	3.3965	1.5458
0.3500	0.0430	0.0083	1.3930	1.9425	1.6721	3.2925	1.3500
0.4000	0.0496	0.0125	1.2338	2.0217	1.9042	3.2059	1.1842
0.4500	0.0556	0.0177	1.0964	2.0907	2.1418	3.1315	1.0408
0.5000	0.0609	0.0239	0.9758	2.1513	2.3859	3.0662	0.9149
0.5500	0.0653	0.0310	0.8683	2.2047	2.6370	3.0077	0.8030
0.6000	0.0687	0.0387	0.7713	2.2519	2.8957	2.9545	0.7026
0.6500	0.0710	0.0469	0.6828	2.2937	3.1624	2.9054	0.6118
0.7000	0.0722	0.0552	0.6013	2.3305	3.4371	2.8597	0.5291
0.7500	0.0720	0.0630	0.5256	2.3629	3.7201	2.8165	0.4536
0.8000	0.0704	0.0700	0.4547	2.3912	4.0112	2.7755	0.3843
0.8500	0.0674	0.0754	0.3880	2.4156	4.3105	2.7362	0.3206
0.9000	0.0628	0.0786	0.3247	2.4363	4.6177	2.6982	0.2619
0.9500	0.0566	0.0787	0.2644	2.4534	4.9326	2.6612	0.2078
1.0000	0.0486	0.0748	0.2067	2.4670	5.2547	2.6250	0.1580
1.0500	0.0389	0.0659	0.1512	2.4771	5.5836	2.5893	0.1122
1.1000	0.0274	0.0508	0.0977	2.4835	5.9186	2.5538	0.0703
1.1500	0.0140	0.0283	0.0461	2.4861	6.2588	2.5182	0.0321
1.2000	−0.0012	−0.0026	−0.0036	2.4847	6.6029	2.4823	−0.0024
1.2500	−0.0182	−0.0431	−0.0513	2.4788	6.9496	2.4457	−0.0331
1.3000	−0.0367	−0.0939	−0.0966	2.4678	7.2963	2.4079	−0.0599
1.3500	−0.0565	−0.1554	−0.1389	2.4510	7.6401	2.3686	−0.0824
1.4000	−0.0769	−0.2267	−0.1770	2.4272	7.9764	2.3270	−0.1001
1.4500	−0.0968	−0.3053	−0.2094	2.3951	8.2986	2.2825	−0.1126
1.5000	−0.1147	−0.3860	−0.2339	2.3531	8.5973	2.2339	−0.1192
1.5500	−0.1285	−0.4601	−0.2476	2.2996	8.8603	2.1805	−0.1191
1.6000	−0.1356	−0.5155	−0.2477	2.2332	9.0725	2.1212	−0.1120
1.6500	−0.1334	−0.5370	−0.2316	2.1532	9.2174	2.0551	−0.0982
1.7000	−0.1196	−0.5087	−0.1980	2.0598	9.2794	1.9815	−0.0783
1.7500	−0.0923	−0.4142	−0.1460	1.9532	9.2439	1.8995	−0.0537
1.8000	−0.0498	−0.2350	−0.0754	1.8333	9.0956	1.8077	−0.0256
1.8500	0.0107	0.0530	0.0155	1.6984	8.8137	1.7032	0.0048
1.9000	0.0938	0.4889	0.1304	1.5444	8.3627	1.5810	0.0366
1.9500	0.2106	1.1514	0.2796	1.3604	7.6672	1.4294	0.0690
2.0000	0.3965	2.2751	0.4980	1.1110	6.4958	1.2125	0.1015
2.0100	0.4536	2.6293	0.5616	1.0415	6.1305	1.1495	0.1080
2.0200	0.5269	3.0859	0.6410	0.9561	5.6623	1.0702	0.1141
2.0300	0.6190	3.6648	0.7370	0.8514	5.0710	0.9694	0.1180
2.0500	0.6577	3.9630	0.7680	0.7842	4.7399	0.8945	0.1103
2.1000	0.6421	4.0289	0.7290	0.7195	4.5218	0.8065	0.0869
2.1500	0.6035	3.9377	0.6690	0.6642	4.3376	0.7297	0.0655
2.2000	0.5495	3.7242	0.5960	0.6071	4.1166	0.6535	0.0465
2.2500	0.4859	3.4173	0.5160	0.5370	3.7777	0.5670	0.0301
2.3000	0.4055	2.9567	0.4220	0.4502	3.2835	0.4667	0.0165

TABLE 2. Parameters of a critical system with non-identical drops suspended from holes of equal radii R^0.

shapes of drops are uniquely determined by the terminal points of the equilibrium profiles. In turn, the terminal points of profiles related to two connected non-identical critical drops are the points of the curves H_1^* and H_2^* with given $R = R^0$. The

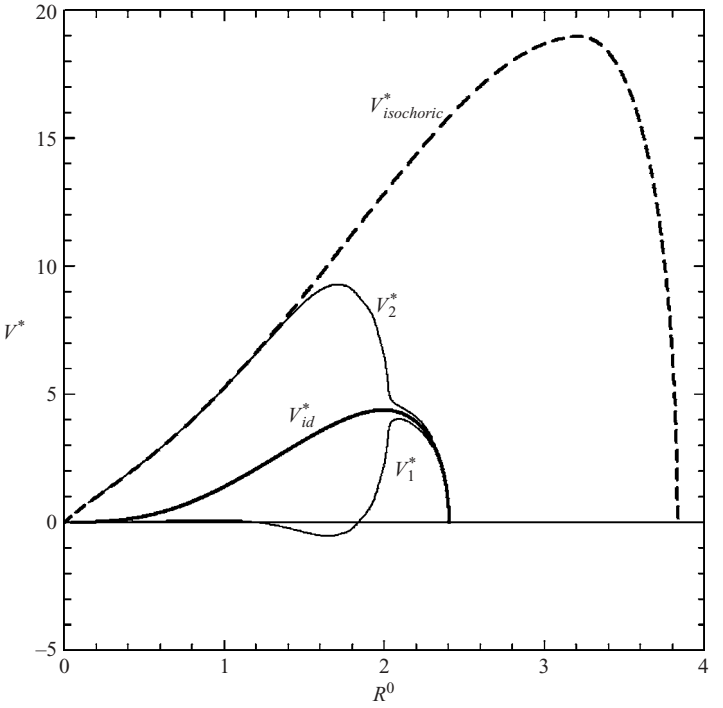

FIGURE 10. Critical dimensionless volume, V^*_{id}, of each identical drop in comparison with critical volumes, V^*_1 and V^*_2, of non-identical drops suspended from edges of holes with equal dimensionless radii, R^0. The dashed line shows the stability limit for a single drop with respect to isochoric perturbations.

distinctive feature of these curves is that they make a sharp approach to the curve H^*_{id} as R^0 exceeds 2.0. On the other hand, as R^0 tends to zero, the curve H^*_2 coincides approximately with (but slightly lower than) the boundary, OtA, of solitary drop stability to IC-perturbations. Another feature of the curves is that H^*_1 is negative for $1.20 < R^0 < 1.84$. This means that the related critical equilibrium surface is convex upwards, and bounds a 'sessile bubble' rather than a 'pendant drop'. Profiles of sessile bubbles correspond to $Q < 0$ and represent a mirror reflection (with respect to the R-axis) of profiles for pendant drops. Thus, for $1.20 < R^0 < 1.84$, the critical system consists of a large pendant drop and a small sessile bubble. The maximum value of the critical height H^*_2 is 2.486 and is achieved at $R^0 = 1.16$. The shape of the related drop is determined by $Q = 2.511$. The minimum value of H^*_1 is -0.136 and corresponds to a bubble with $R^0 = 1.61$ and $Q = -0.246$.

As in the cases of a solitary drop and a system of connected identical drops, the dimensionless protruded volume is the most prominent integral characteristic of stability for a system of non-identical drops. Notice that the protruded volume is bounded by a drop free surface and the plane of the hole. For a sessile bubble, the volume is withdrawn into the bulk liquid side of the plate and is negative. As indicated above, the solid line in figure 3 may be considered as representing the dependence of the critical dimensionless volume of each of identical pendant drops on the dimensionless hole radius. In addition to the curves already shown in figure 3, figure 10 depicts the critical volumes, V^*_1 and V^*_2, for non-identical drops.

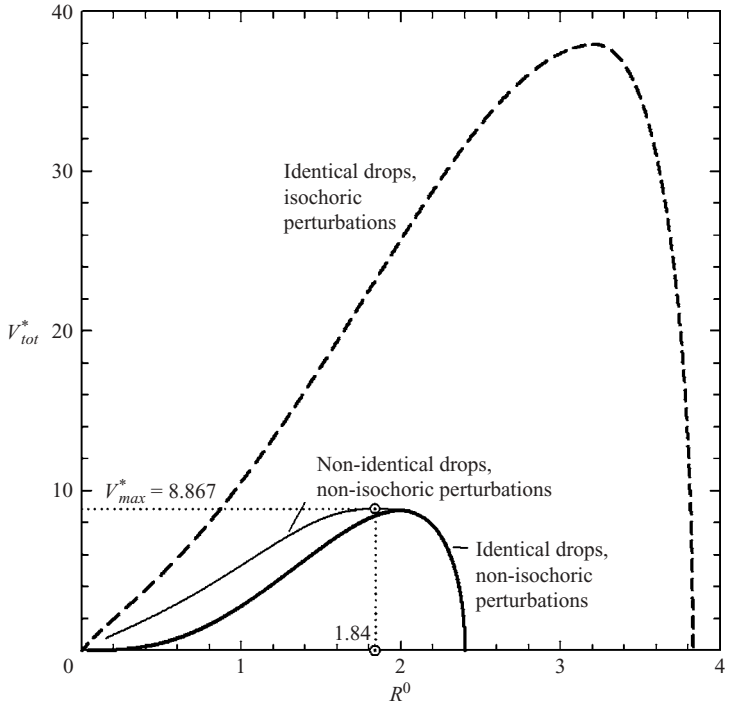

FIGURE 11. Total critical volume for identical and non-identical drops under non-isochoric perturbations (solid lines) and for identical drops under isochoric perturbations (dashed line).

The maximum value of the critical volume V_2^* was found to be 9.281 (the drop with $R^0 = 1.71$ and $Q = 1.966$), while the minimum value of V_1^* is -0.537 ($R^0 = 1.65$, $Q = -0.232$). Although the curves $V^*_{isochoric}$ and V_2^* in figure 10 appear as merged at small values of R^0, it should be emphasized that the larger of the two non-identical drops has a critical volume that is always less than the critical volume for a solitary drop subject to IC-perturbations.

The two-drop stability is best characterized by the total protruded dimensional liquid volume, $V_{tot} = V_1 + V_2$. The thick solid line in figure 11 depicts a critical total volume for identical drops that is twice the critical volume for each of the identical drops (see figure 10). The thin solid line shows the stability limit for non-identical drops and represents the sum, $V_1^* + V_2^*$, of critical volumes already shown in figure 10. Despite the fact that the total critical volume for non-identical drops always exceeds that for identical drops, both the solid lines practically merge when R^0 exceeds 2.0. As shown in figure 11, the maximum value of $V_1^* + V_2^*$ for non-identical drops is 8.867, and occurs when $R^0 = 1.84$. For IC-perturbations, the critical volume for a solitary drop hanging from the hole of the same radius ($R^0 = 1.84$) is 11.578. For $1.16 \leqslant R^0 \leqslant 2.4048$, the maximum volume for an IC-stable solitary drop is always greater than the maximum total volume for a stable system of two connected drops suspended from holes of the same radius R^0. The dashed line in figure 11 corresponds to the case when NI-perturbations are ignored. Then the critical system would consist of two identical drops critical to IC-perturbations, and the total critical volume would be twice the critical volume for a solitary drop under IC-perturbations.

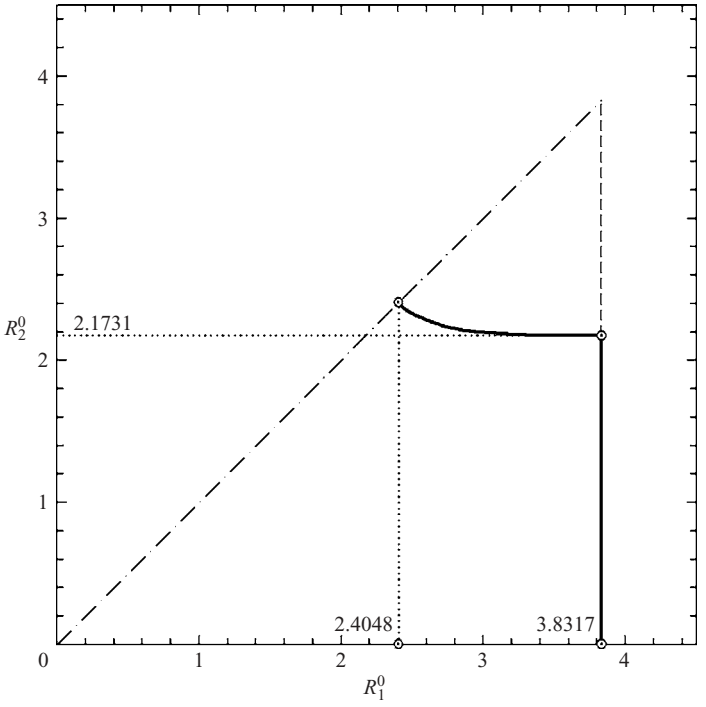

FIGURE 12. Stability boundary (solid lines) for a system of two drops with horizontal free surfaces (after Slobozhanin 1983). (Our assumption that $R_1^0 \geqslant R_2^0$ restricts the region of interest.)

5. Effect of gravity: drops hanging from unequal radii holes

First we report the known results related to the simplest case of flat free surfaces ($Q_1 = Q_2 = 0$) pinned to edges of holes in the plate. These results are required as a starting point for the bifurcation analysis described in the subsequent subsections where we consider stable drops with horizontal free surfaces as initial shapes for connected drops with curved free surfaces. For unequal radii holes, $R_2^0 < R_1^0$, there are three intervals of the larger radius values, $0 < R_1^0 < 2.4048$, $2.4048 < R_1^0 < 3.219$ and $3.219 < R_1^0 < 3.8317$, within which the stability characteristics for systems with curved surfaces have similar properties. Each of these intervals is examined and discussed in the following subsections.

5.1. *Horizontal free surfaces*

When both drops are bounded from below by horizontal free surfaces ($Q_i = 0$, $Z_i \equiv 0$, $R_i \equiv S_i$) pinned to edges, the condition (12) of the stability to NI-perturbations assumes the form (Slobozhanin 1983)

$$D_0 \equiv \tfrac{1}{2}\left(R_1^{0^2} + R_2^{0^2}\right) J_0\left(R_1^0\right) J_0\left(R_2^0\right) - R_1^0\, J_0\left(R_2^0\right)\, J_1\left(R_1^0\right) - R_2^0\, J_0\left(R_1^0\right)\, J_1\left(R_2^0\right) < 0. \quad (28)$$

When IC-perturbations are taken into account, the supplementary restriction,

$$R_1^0 < 3.8317, \quad (29)$$

must be applied to ensure stability. Thus, the inequalities (28), (29) provide the conditions for stability to arbitrary perturbations. This stability region is shown in figure 12. The curve $D_0 = 0$ and the vertical line $R_1^0 = 3.8317$ intersect at the point with

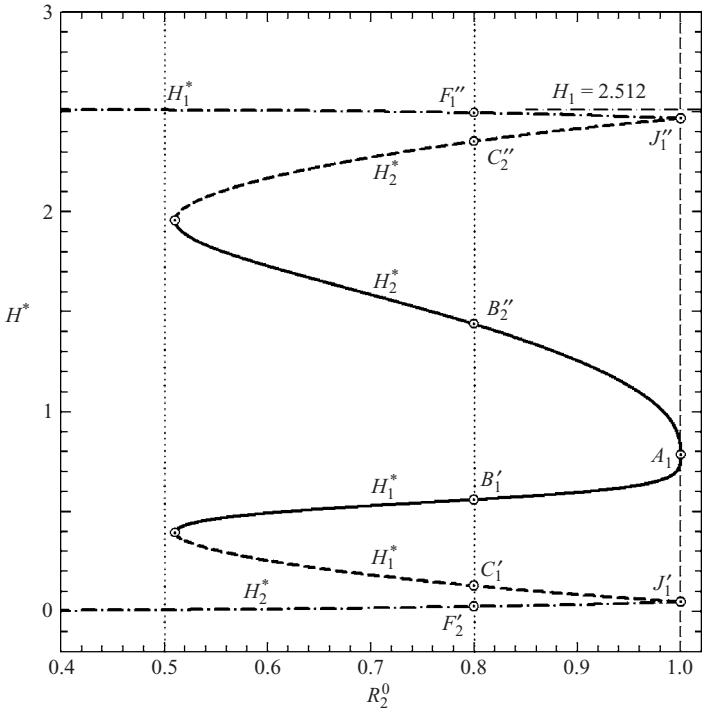

FIGURE 13. Dimensionless heights H_1^* and H_2^* of connected NI-critical drops suspended from holes of radii $R_1^0 = 1$ and R_2^0 as functions of the smaller hole radius, R_2^0. For a given R_2^0, critical states are determined by the points on solid segments, dashed segments, and dot-dash segments.

$R_2^0 = 2.1731$. The curve $D_0 = 0$ and dot-dash line $R_1^0 = R_2^0$ intersect at the point $R_1^0 = R_2^0 = 2.4048$ which determines the stability limit for equal diameter holes, as was mentioned above. Thus, for $0 < R_2^0 < 2.1731$, loss of stability occurs with respect to non-axisymmetric perturbations (when R_1^0 exceeds 3.8317). If $2.1731 < R_2^0 < 2.4048$, NI-perturbations become the most dangerous. Finally, if $R_2^0 > 2.4048$, systems with horizontal free surfaces become unstable (this is consistent with conclusion (ii) in § 1.2). For plane free surfaces Γ_1 and Γ_2, the critical sizes of the holes are greater than those for curved surfaces. Thus, the critical radii determined by (28) and (29) are the maximum possible radii of holes for any stable equilibrium of two connected suspended drops.

5.2. *Systems with* $0 < R_1^0 < 2.4048$

We first consider the case $R_1^0 = 1$. A verification of the stability condition (12) for two drops related by the equal reference pressures constraint (27) allows us to find systems critical to NI-perturbations with a fixed radius $R_1^0 = 1$ of the larger hole and a variable radius R_2^0 of the smaller hole. The heights of drops for such systems are shown in figure 13. First in our calculations we proceed from the point A_1 (figure 13) which corresponds to a system of two identical critical drops with equal radii holes $R_1^0 = R_2^0 = 1$. This system also corresponds to the point A_1 in figures 7–8. From this starting position, the system parameters are varied so that a continuous extension of critical systems in the direction of $R_2^0 < 1$ is obtained. In this extension, for $R_1^0 = 1$,

there is a local minimum $R_2^0 = 0.5106$. Further variation of the system parameters leads to the bending of the neutral stability curve and this leads to the second branch of critical states. The first and second branches are shown as solid and dashed lines, respectively, in figure 13. Both branches exist for $0.5106 < R_2^0 \leqslant 1$. The point of intersection of the second branch with the line $R_2^0 = 1$ determines the second critical state for the system with $R_1^0 = R_2^0 = 1$. This state corresponds to critical non-identical drops and is determined by the points J_1' and J_1'' in figure 7. Since $H_2^* > H_1^*$ along the second branch, this state is also the lower ($V_1 - V_2 < 0$) of the two symmetrical critical states shown in figure 8.

For $R_1^0 = R_2^0 = 1$, states that correspond to points within the segments A_1J_1' and A_1J_1'' are stable. Likewise, for $0.5106 < R_2^0 < 1$, states determined by points that lie within segments bounded by two branches of critical states are stable to NI-perturbations. For example, for $R_2^0 = 0.8$, these segments are $C_1'B_1'$ and $C_2''B_2''$ in figure 13. It should be emphasized that the value H_2^* along the second branch is less than the IC-critical value for a solitary drop 2 with a radius $R^0 = R_2^0$. It follows that NI-perturbations are the most dangerous along both branches.

There exists another family of states critical to NI-perturbations. It proceeds from the critical state for $R_1^0 = R_2^0 = 1$ (determined by the points J_1' and J_1'' in figure 7) and by the upper ($V_1 - V_2 > 0$) of the two symmetrical critical states shown in figure 8. For this family, $H_1^* > H_2^*$. This third branch of critical states exists for $0 < R_2^0 \leqslant 1$. The H_1^* value increases monotonically as R_2^0 decreases, and tends to the value 2.512 as $R_2^0 \to 0$. This value corresponds to a solitary drop 1 (with $R_1^0 = 1$) critical to IC-perturbations. The value of H_2^* decreases as R_2^0 decreases and tends to zero as $R_2^0 \to 0$. Thus, for any $0 < R_2^0 \leqslant 1$, the loss of stability occurs with respect to NI-perturbations rather than losing stability because drop 1 becomes IC-unstable.

To gain greater insight into the effect of the value of R_2^0, we constructed the bifurcation diagrams for different R_2^0 to account for IC-perturbations and NI-perturbations. First, we consider R_2^0 values in the interval $0.5106 < R_2^0 < 1$.

Figure 14 shows two curves that originate at (0,0). Each curve is associated with a family of drops designated as family 1 (lower curve) and family 2 (upper curve). The drops in family 1 hang from holes of radius $R_1^0 = 1$ and those of family 2 hang from holes with radius $R_2^0 = 0.8$. According to conclusion (i) (§ 1.2), the correspondences shown in figure 14(*a*) determine the branch of stable equilibrium states of two connected drops. It is marked as branch I in figure 15. Correspondences (see figure 14*b*) between points of the segments A_1F_1'' (family 1) and $A_2'F_2'$ (family 2) also determine stable states for pairs of connected drops. They belong to the branch II – 1 in figure 15. The coupled drops corresponding to the points F_1'' and F_2' are NI-critical (see also these same drops marked as $F_1''$and F_2' in figure 13). Correspondences between CP-stable solitary drops of family 2 and IC-unstable solitary drops of family 1 beyond the stability limit to NI-perturbations are also illustrated by dotted lines in figure 14(*b*). These correspondences determine states of pairs of drops on the branch II – 2 in figure 15. States on this branch are NI-unstable. The terminus of this branch is shown as a filled circle and corresponds to the arbitrarily chosen pair of drops $I_2' - I_1''$. Thus, pairs of drops consisting of a CP-stable solitary drop from family 2 and a CP-unstable solitary drop from family 1 may be stable (branch II – 1) or unstable (branch II – 2). The loss of collective stability to NI-perturbations occurs before the solitary drop of family 1 becomes critical to IC-perturbations. The critical system serves as a turning point on the bifurcation diagram. In contrast, for zero-gravity (see branch *Ak* in figure 5), a pair of drops consisting of a CP-unstable drop from family 1 and a CP-stable drop from family 2 is always stable.

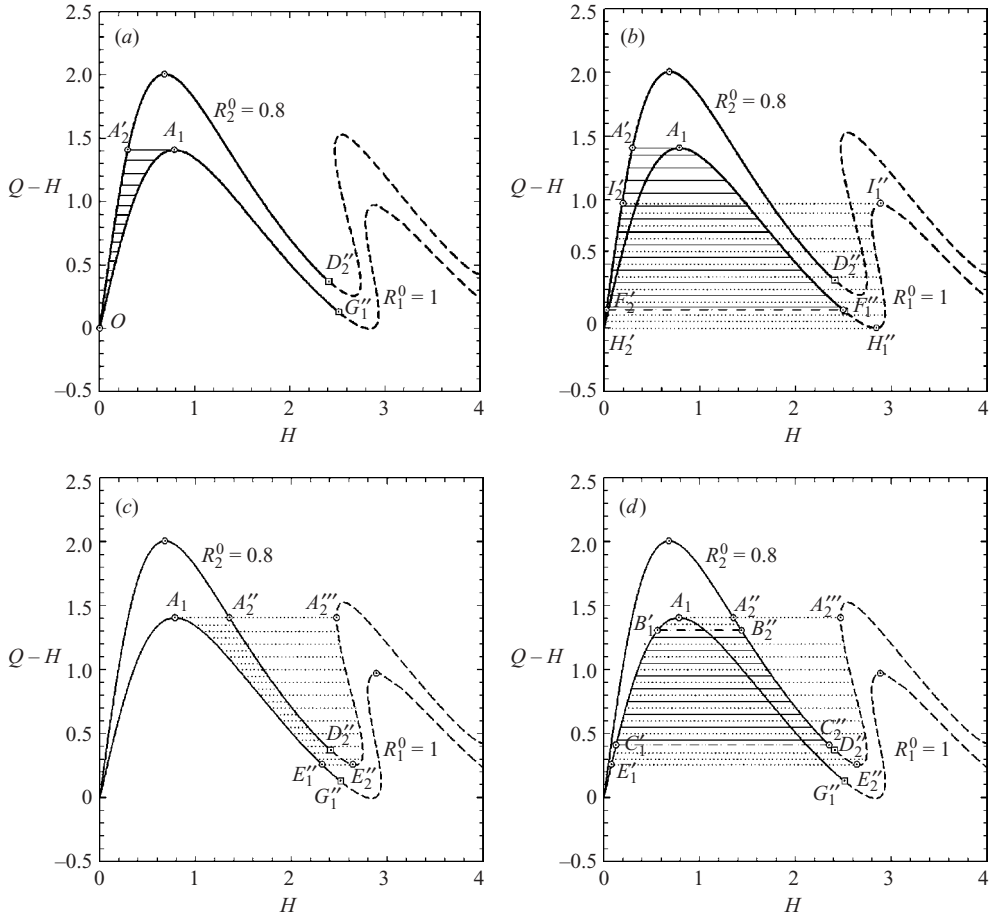

FIGURE 14. Dependence of the dimensionless reference pressure $(Q-H)$ on H for drops with free surfaces pinned to edges of holes with radii $R_1^0=1$ and $R_2^0=0.8$. Points of solid (dashed) segments correspond to solitary IC-stable (IC-unstable) drops. Horizontal straight lines establish correspondence between two drops with equal reference pressures. Thin solid lines correspond to pairs of stable connected drops; dotted lines – to unstable connected drops; and dot-dash lines to critical systems of connected drops. Correspondences are grouped together by stability or instability of solitary drops of families 1 ($R_1^0=1$) and 2 ($R_2^0=0.8$) to CP-perturbations. (*a*) Branch I ($OA_2'-OA_1$). Drops of families 1 and 2 are CP-stable. (*b*) Branch II-1 ($A_2'F_2'-A_1F_1''$); Branch II-2 ($F_2'H_2'I_2'-F_1''H_1''I_1''$). Drops of the family 2 are CP-stable and drops of the family 1 are CP-unstable. (*c*) Branch III ($A_1E_1''A_1-A_2''E_2''A_2'''$) Drops of families 1 and 2 are CP-unstable. (*d*) Branch IV-1 ($A_1B_1'-A_2''B_2''$); branch IV-2 ($B_1'C_1'-B_2''C_2''$); branch IV-3 ($C_1'E_1'A_1-C_2''E_2''A_2'''$) Drops of the family 1 are CP-stable and drops of the family 2 are CP-unstable.

Correspondences shown in figure 14(*c*) between CP-unstable solitary drops determine states of pairs of drops that are definitely unstable according to conclusion (ii) of § 1.2. These states correspond to the points of branch III in figure 15. The initial point on the bifurcation diagram (the boundary point between segments III and IV – 1) corresponds to the pair of drops A_1-A_2''. The remainder of branch III corresponds to the pairs resulting from moving along the family 2 from the drop A_2'' to the drop A_2''' (figure 14*c*). The terminal point of branch III shown as a filled circle corresponds to the pair A_1-A_2'''. Branch III is a continuous curve, part of which lies outside the

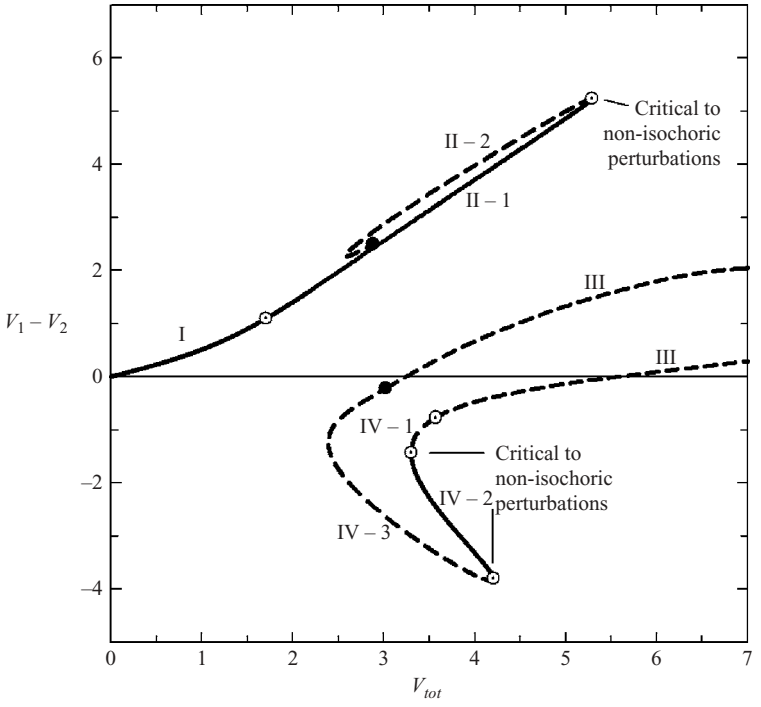

FIGURE 15. Bifurcation diagram for two connected drops suspended from holes of radii $R_1^0 = 1$ and $R_2^0 = 0.8$. Solid (dashed) lines correspond to stable (unstable) states.

field of figure 15. Here the curve bends upward, the value of V_{tot} reaches its maximum, and the curve turns back.

Branch IV is associated with pairs of drops, one drop from family 1 that is CP-stable and one drop from family 2 that is CP-unstable (figure 14*d*). Correspondences are established from drop A_2'' to drop A_2''' along family 2. The pairs of drops from the segments $A_2''B_2''$ and A_1B_1' are presented as the segment IV – 1 on the bifurcation diagram in figure 15. Like states of the branch III, these systems are unstable. Stability is restored for pairs of drops that correspond to interior points of the segments $B_2''C_2''$ and $B_1'C_1'$ (figure 14*d*). These are just the stable states described above and shown in figure 13 at $R_2^0 = 0.8$. Attention is drawn to the fact that solitary drops related to these states are also IC-stable (the solitary drop from family 2 critical to IC-perturbations corresponds to the point D_2'' in figure 14*d*). On the bifurcation diagram, these states correspond to the interior points of the segment IV – 2, while critical states are the turning points. Finally, drops of family 2 that are presented as points of the segment $C_2''D_2''E_2''A_2'''$ (figure 14*d*) and corresponding drops of family 1 (the segment $E_1'A_1$) form pairs that are unstable (the branch IV – 3 on the bifurcation diagram). In comparison to the case of zero-gravity (branch *Cn* of figure 5) the lower segment of stable states (segment IV – 2 in figure 15) is no longer semi-infinite but is bounded by two turning points on the bifurcation diagram.

If $R_2^0 < 0.5106$, then according to figure 13 the stable states on the lower segment of the bifurcation diagram should disappear. To gain a better understanding of the evolution of this segment, equal reference pressure correspondences were established not only between families of drops hanging from holes of radii $R_1^0 = 1$ and $R_2^0 = 0.8$, but also between drops hanging from holes of radii $R_1^0 = 1$ and $R_2^0 = 0.5$, 0.4 and 0.3

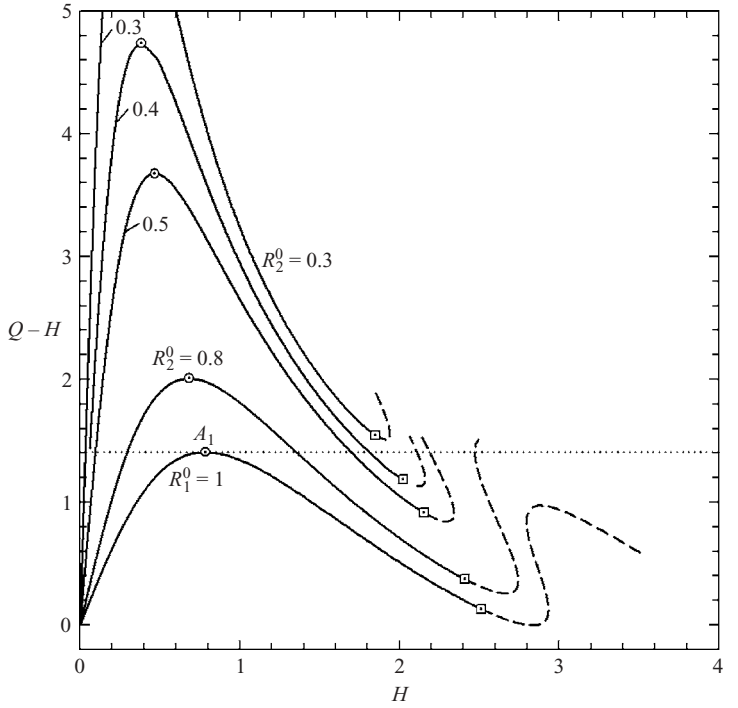

FIGURE 16. Dimensionless reference pressure, $(Q - H)$, as a function of H for $R_1^0 = 1$ and a set of R_2^0 values. The dot-centred squares on each curve separate IC-stable (solid line) and IC-unstable (dashed line) solitary drops. The dot-centred circles correspond to the maximum values of $(Q - H)$. The horizontal dotted line indicates this value for $R_1^0 = 1$.

(figure 16). We truncated the curves for $R_2^0 = \text{const}$ at points that lie above the dotted line (the maximum $(Q - H)$ value for $R_1^0 = 1$) because the remainders of these curves are of no interest.

Bifurcation diagrams for $R_1^0 = 1$and new values of R_2^0 were constructed and compared with the case $R_1^0 = 1$, $R_2^0 = 0.8$ (figure 17). Branches I, II – 1 and II – 2 for new values of R_2^0 are similar to those for $R_2^0 = 0.8$. Only branches I and II – 1 for $R_2^0 = 0.5$ are shown in figure 17. Critical states and branches II – 2 almost coincide for $R_2^0 = 0.8$ and for $R_2^0 = 0.5$. For $R_2^0 = 0.4$ and 0.3, the branches I and II – 1 are not plotted because they lie very close to those shown for $R_2^0 = 0.5$.

For $R_2^0 = 0.8$ and for new values of R_2^0, branches III and IV are distinctly different. They are separated by points depicted as dot-circles and filled-circles in figure 17. We see that the segment IV – 2 of stable states does not exist for $R_2^0 = 0.5$, and $R_2^0 = 0.4$. Thus, for $R_2^0 < 0.5106$, all states of the branches III and IV become unstable to NI-perturbations. This means that the stability limits with respect to IC-perturbations for solitary drops hanging from a hole of radius R_2^0 and shown by dot-square points in figure 17 do not affect our conclusions regarding the instability of branches III and IV to arbitrary perturbations. Furthermore, branches III and IV shrink as R_2^0 decreases and eventually disappear. For example, there are no branches III and IV for $R_2^0 = 0.3$ because all CP-unstable solitary drops hanging from a hole of radius $R_2^0 = 0.3$ have a reference pressure value, $Q - H$, that is greater than the maximum value for $R_1^0 = 1$ (see figure 16). Thus, the related correspondences and, consequently, the equilibria are impossible.

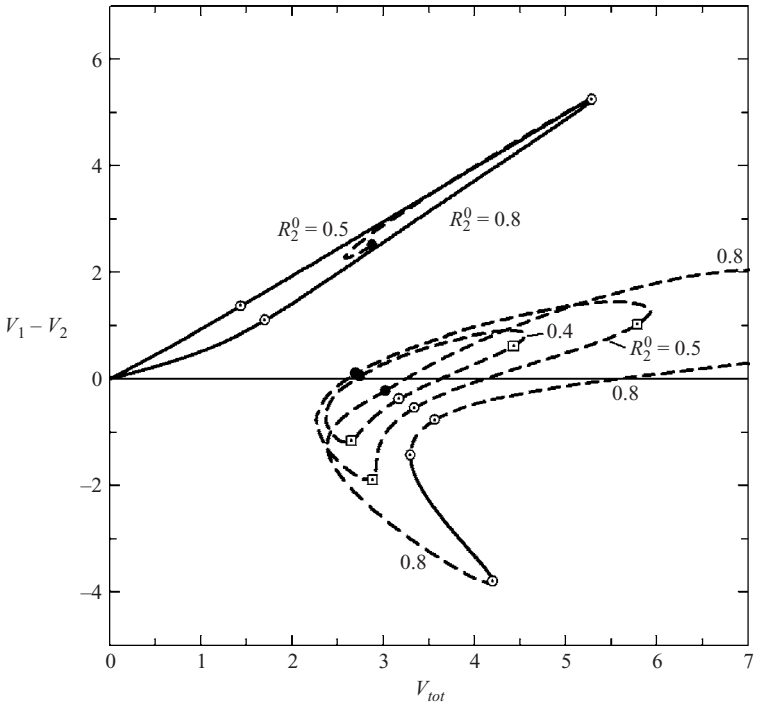

FIGURE 17. Evolution of the bifurcation diagrams for $R_1^0 = 1$ as the smaller hole radius, R_2^0, changes. Solid (dashed) lines correspond to stable (unstable) states.

We have analysed the case of $R_1^0 = 1$. For other values of R_1^0 from the interval $0 < R_1^0 < 2.4048$, the situation is quite similar. The stable systems are universally present (like those represented by branches I and II – 1 in figure 15) and are bounded by the NI-critical state. Another branch of stable states (similar to that presented by the segment IV – 2 in figure 15) exists if the radii R_2^0 and R_1^0 values are sufficiently close. This branch is bounded by two states critical to NI-perturbations (in total, we have three NI-critical states). What is the minimum R_2^0 value with these stable states for a prescribed R_1^0? For R_1^0 from the interval $0.2 \leqslant R_1^0 \leqslant 2.0$, these values, $R_{2\,min}^0$, are given in table 3. If $0 < R_1^0 \leqslant 0.15$, the value of $R_{2\,min}^0$ is less than 0.005. On the other hand, for $2.05 \leqslant R_1^0 < 2.4048$, the difference $R_1^0 - R_{2\,min}^0$ is less than 0.0001.

5.3. *Systems with* $2.4048 < R_1^0 < 3.219$

According to conclusions (i) and (ii) in § 1.2, if $2.4048 < R_1^0 < 3.8317$, stable and critical states may exist only for $R_2^0 < 2.4048$. First, we consider the case of $R_1^0 = 3$ that is typical for $2.4048 < R_1^0 < 3.219$. As becomes apparent from the analysis of the stability of two connected 'drops' with horizontal free surfaces (§ 5.1), the system with $R_1^0 = 3$ may be stable only if $R_2^0 < 2.1954$.

It follows from figure 6 that an IC-stable solitary drop hanging from the hole with $R^0 = 3$ has a non-positive reference pressure, whereas IC-stable solitary drops hanging from the holes with $R^0 = 0.5$ and 1 have non-negative reference pressures. To establish the equal reference pressure correspondence for the system with two holes, $R_1^0 = 3$ and $R_2^0 = 0.5$ or $R_2^0 = 1$, we must replace one of the pendant drops with a sessile bubble. For the sake of definiteness, we will always assume that a free surface in contact with

R_1^0	$R_{2\,min}^0$	R_1^0	$R_{2\,min}^0$	R_1^0	$R_{2\,min}^0$
0.20	0.0055	0.85	0.3368	1.50	1.2446
0.25	0.0107	0.90	0.3911	1.55	1.3264
0.30	0.0182	0.95	0.4491	1.60	1.4093
0.35	0.0285	1.00	0.5106	1.65	1.4926
0.40	0.0419	1.05	0.5750	1.70	1.5758
0.45	0.0585	1.10	0.6421	1.75	1.6577
0.50	0.0787	1.15	0.7115	1.80	1.7369
0.55	0.1027	1.20	0.7828	1.85	1.8119
0.60	0.1307	1.25	0.8560	1.90	1.8811
0.65	0.1630	1.30	0.9308	1.95	1.9437
0.70	0.1997	1.35	1.0072	2.00	1.9994
0.75	0.2409	1.40	1.0849		
0.80	0.2867	1.45	1.1641		

TABLE 3. Minimum values of the smaller hole radius, R_{2min}^0, at which three NI-critical states exist for given values of the larger hole radius R_1^0.

edges of the greater hole (with radius R_1^0) is the surface of a pendant drop. When a pendant drop is replaced with a corresponding sessile bubble, the substitution $Q \to -Q$, $H \to -H$, $V \to -V$ should be performed. Then a curve shown in figure 6 for pendant drops is replaced with the curve symmetric with respect to the origin. According to the calculation, for any R_2^0 from the interval $0 < R_2^0 < 2.1954$, stable and critical systems may exist only if a surface pinned to edges of the smaller hole is a sessile bubble surface. Figure 18 shows the curves $(Q - H)$ *vs.* H for pendant drops with $R_1^0 = 3$ and for sessile bubbles with $R_2^0 = 2$, 1.5 and 1. For each pair of the R_1^0 and R_2^0 values, we proceed from the stable configuration consisting of two horizontal free surfaces and corresponding to the point O in figure 18 and move in the direction of the decreasing $(Q - H)$ value. Since all solitary drops hanging from the hole with $R_1^0 = 3$ are CP-unstable, pairs of drops may be NI-stable only if the sessile bubbles are CP-stable (see conclusions (i) and (ii) in § 1.2). This means that they must lie on the segment of the corresponding R_2^0 curve bounded by the point O and the minimum point of $(Q - H)$ (figure 18). Critical states are determined by NI-perturbations and are shown as those corresponding to the points A_1 and A_2, B_1 and B_2, C_1 and C_2, respectively. The shapes of these critical configurations are shown in figure 19. Note that solitary pendant drops and sessile bubbles that form critical systems are IC-stable. In particular, this is also true for the pendant drop corresponding to the point C_1in figure 18. The bifurcation diagrams shown in figure 20 indicate that the critical systems represent turning points.

In the examples described above, we have analysed the systems with $R_1^0 = 3$ and three selected values of R_2^0. Characteristics of the critical systems as the functions of R_2^0, $0 < R_2^0 < 2.1954$, are depicted in figures 21 and 22. In particular, for $R_2^0 = 2$, 1.5 and 1, they are shown as the dot-circle points. For the critical system, as $R_2^0 \to 0$, the drop hanging from the hole with $R_1^0 = 3$ approaches a solitary IC-critical drop. The latter has $H_1 = 2.276$ and $V_1 = 18.693$. In fact, the parameters H_1^* and V_1^* vary only slightly for $R_2^0 < 1$. The extreme right-hand point with $R_2^0 = 2.1954$ corresponds to the critical system consisting of two horizontal flat surfaces. Such a system served as a starting point in our calculations of critical systems with curved free surfaces. The corresponding point separates the critical characteristics H_1^* and H_2^*, V_1^* and V_2^* in figures 21 and 22.

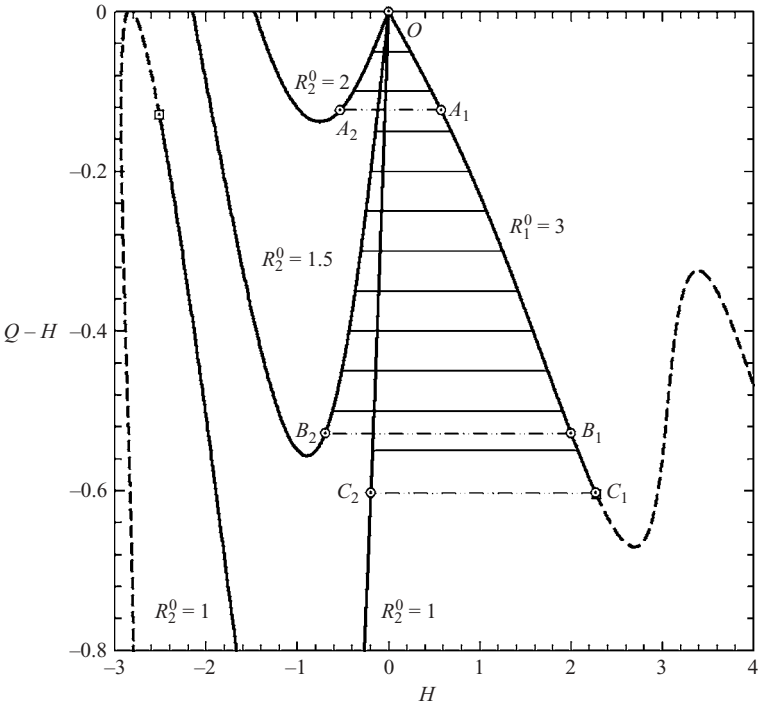

FIGURE 18. Reference pressure for drops hanging from the hole of the radius $R_1^0 = 3$ and for bubbles resting on edges of holes with smaller radii, $R_2^0 = 2$, 1.5 and 1. Thick solid lines correspond to IC-stable and dashed lines correspond to IC-unstable solitary drops or bubbles. Thin horizontal lines establish the correspondences between connected drops and bubbles. Thin solid lines and dot-dash lines indicate stable systems and critical systems, respectively.

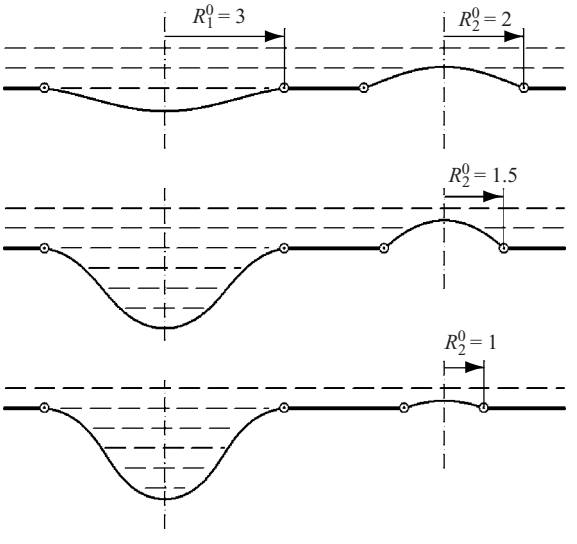

FIGURE 19. Shapes of critical configurations for $R_1^0 = 3$ and different values of R_2^0.

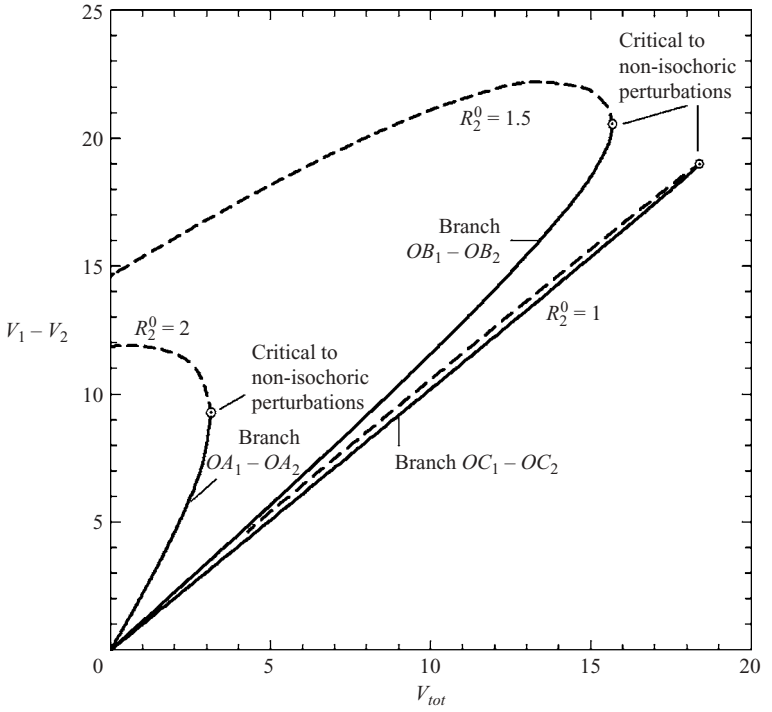

FIGURE 20. Bifurcation diagrams for the systems with the larger hole radius $R_1^0 = 3$ and the smaller hole radii $R_2^0 = 2$, 1.5, and 1. Solid (dashed) lines correspond to stable (unstable) states.

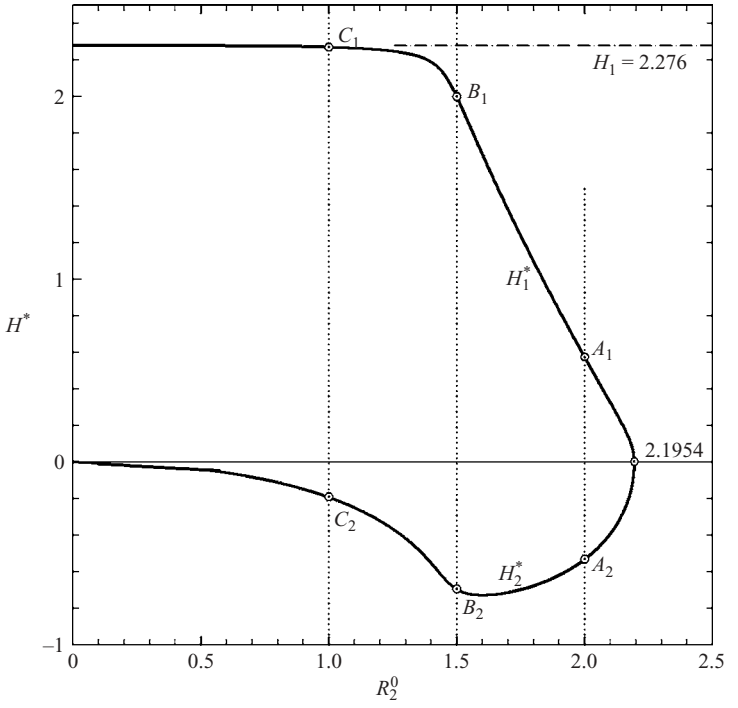

FIGURE 21. Heights of a pendant drop, H_1^*, and a sessile bubble, H_2^*, for critical systems with the larger hole radius $R_1^0 = 3$ as functions of the smaller hole radius, R_2^0.

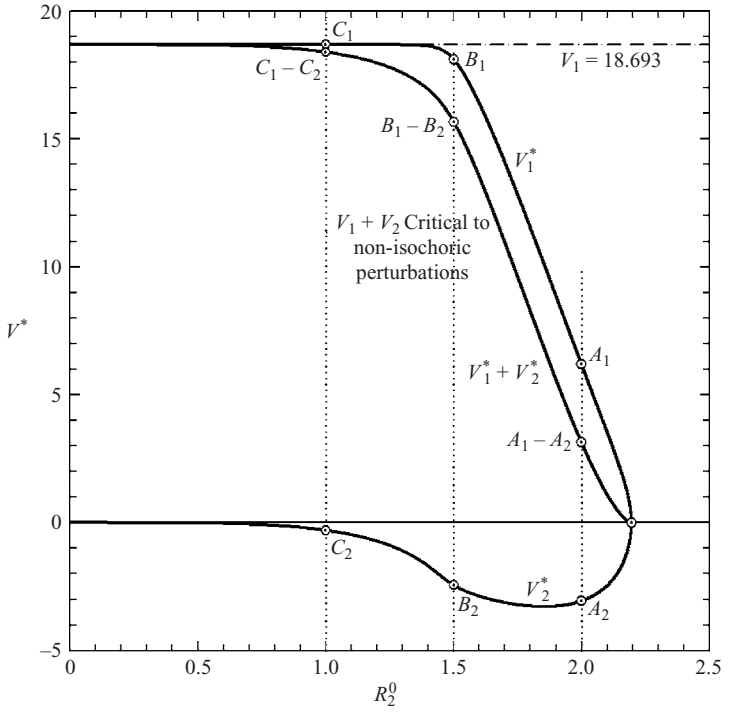

FIGURE 22. Protruded volumes for critical systems with $R_1^0 = 3$ and variable smaller hole radius, R_2^0.

Similar calculations were also performed for the cases $R_1^0 = 2.5$ and 2.75. The results obtained were qualitatively identical to those described above for the case $R_1^0 = 3$.

5.4. *Systems with* $3.219 < R_1^0 < 3.8317$

Here, as in the interval $2.4048 < R_1^0 < 3.219$ considered above, for a fixed R_1^0 the NI-critical system tends, as $R_2^0 \to 0$, to the system with drop 1 (with R_1^0) critical to axisymmetric IC-perturbations. The distinctive feature of the interval $3.219 < R_1^0 < 3.8317$, as noted in § 1.1, is that non-axisymmetric perturbations (always isochoric) for the solitary drop 1 are more dangerous than axisymmetric IC-perturbations. This means that non-axisymmetric perturbations of drop 1 also become more dangerous in comparison to NI-perturbations of a pair of connected drops for relatively small values of R_2^0. We first illustrate the stability of the systems with $3.219 < R_1^0 < 3.8317$ using $R_1^0 = 3.5$.

Figure 23 shows correspondences between drops hanging from holes of $R_1^0 = 3.5$ and bubbles resting on edges of holes with $R_2^0 = 2$, 1.5 and 1. For comparison, the reference pressure curve for $R_1^0 = 3$ and the critical states B_1,B_2 and C_1, C_2 for systems with $R_1^0 = 3$ and $R_2^0 = 1.5$ and 1 previously shown in figure 18 are included in figure 23. Again, as in the case of $R_1^0 = 3$, we proceed from the stable configuration with horizontal free surfaces (the point O) and move in the direction of decreasing reference pressure. The states critical to NI-perturbations for $R_1^0 = 3.5$ and $R_2^0 = 2$, 1.5 and 1, correspond to the points D_1 and D_2, F_1 and F_2, and G_1 and G_2, respectively. However, NI-perturbations do not determine the stability limit in the cases of $R_2^0 = 1.5$

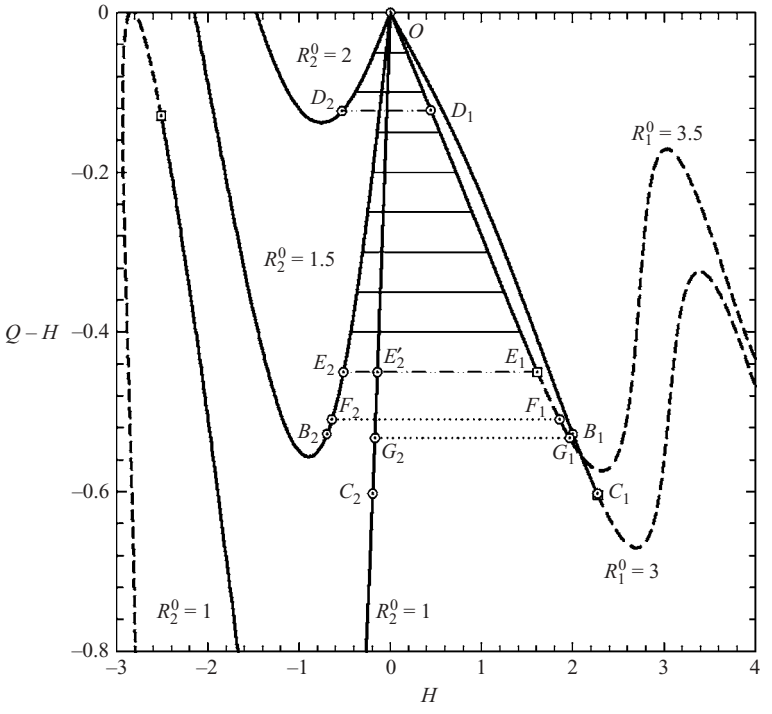

FIGURE 23. Reference pressure, $Q - H$, as a function of H for pendant drops with $R_1^0 = 3.5$ and 3, and for sessile bubbles with $R_2^0 = 2$, 1.5 and 1. Solid (dashed) segments correspond to IC-stable (IC-unstable) solitary drops or bubbles. Horizontal lines show equal reference pressure correspondences between pendant drops with $R_1^0 = 3.5$ and sessile bubbles. Thin solid lines and dot-dashed lines indicate stable systems and critical systems, respectively.

and 1. Indeed, drops hanging from hole of $R_1^0 = 3.5$ and corresponding to the points F_1 and $G_1$are already unstable to non-axisymmetric perturbations. The solitary drop 1 critical to non-axisymmetric perturbations corresponds to the point E_1. Thus, the stability limits for the cases $R_2^0 = 1.5$ and 1 are determined by the systems of two drops corresponding to the points E_1 and E_2, and E_1 and E_2', respectively.

When determined by NI-perturbations, the stability limit is a regular turning point in the total volume (see the bifurcation diagram for $R_2^0 = 2$ in figure 24). However, the nature of the bifurcation undergoes a change when loss of stability occurs to non-axisymmetric perturbations ($R_2^0 = 1.5$ and 1). Then the critical system is no longer a turning point. A subcritical bifurcation (like that for a family of solitary drops with the most dangerous non-axisymmetric perturbations) is expected if a bifurcating family of unstable non-axisymmetric drops 1 is constructed.

For $R_1^0 = 3.5$, figures 25 and 26 show the basic characteristics of critical systems as functions of the smaller hole radius, R_2^0. Here the maximum possible value of R_2^0 for a critical state is 2.1743 (the case of horizontal free surfaces). These characteristics are similar for other values of R_1^0, $3.219 < R_1^0 < 3.8317$. Thus, for a given value of R_1^0, there is a particular value of R_2^0 that is a 'crossover' point where the most dangerous perturbations change from non-isochoric (NI) to non-axisymmetric perturbations. For $R_1^0 = 3.5$, the critical system corresponding to this crossover point has $R_2^0 = 1.5835$ (see figure 25). The values of basic parameters for the crossover critical systems corresponding to a set of R_1^0 are shown in table 4.

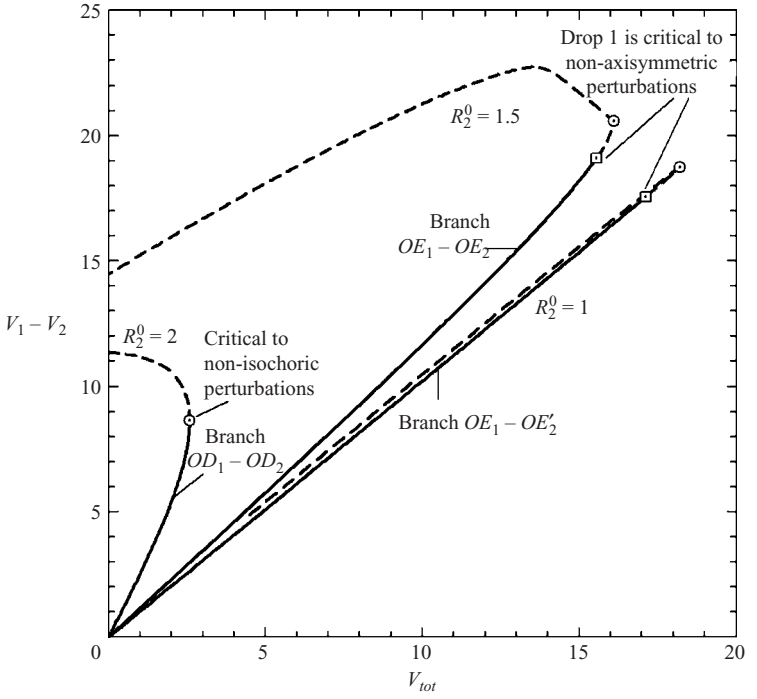

FIGURE 24. Bifurcation diagrams for systems with the larger hole of radius $R_1^0 = 3.5$ and the smaller hole of radii $R_2^0 = 2$, 1.5, and 1. Solid (dashed) segments correspond to stable (unstable) systems.

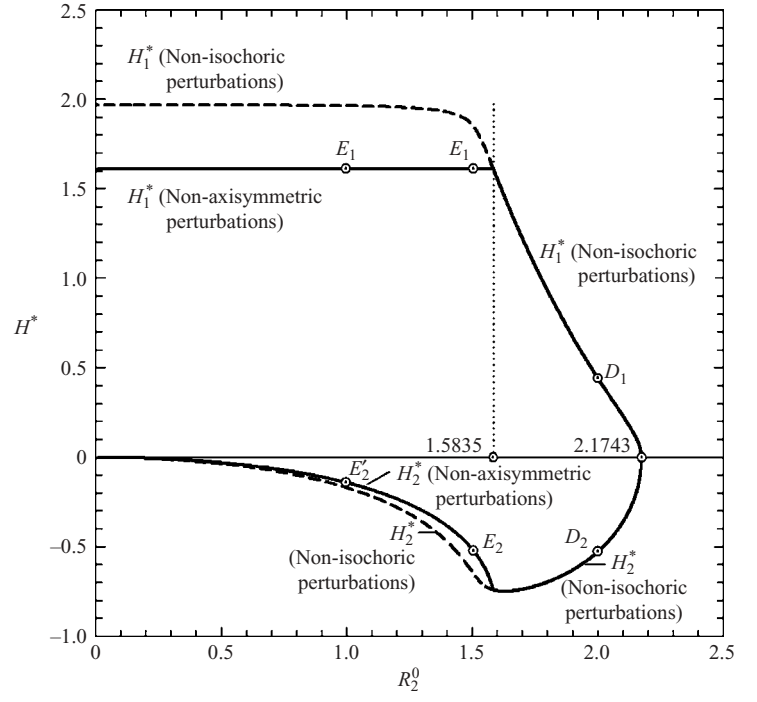

FIGURE 25. Pendant drop height, H_1^*, and a sessile bubble height, H_2^*, for critical systems with a larger hole radius $R_1^0 = 3.5$ and variable smaller hole radius R_2^0. The point designations for $R_2^0 = 2$, 1.5 and 1 are the same as in figure 23.

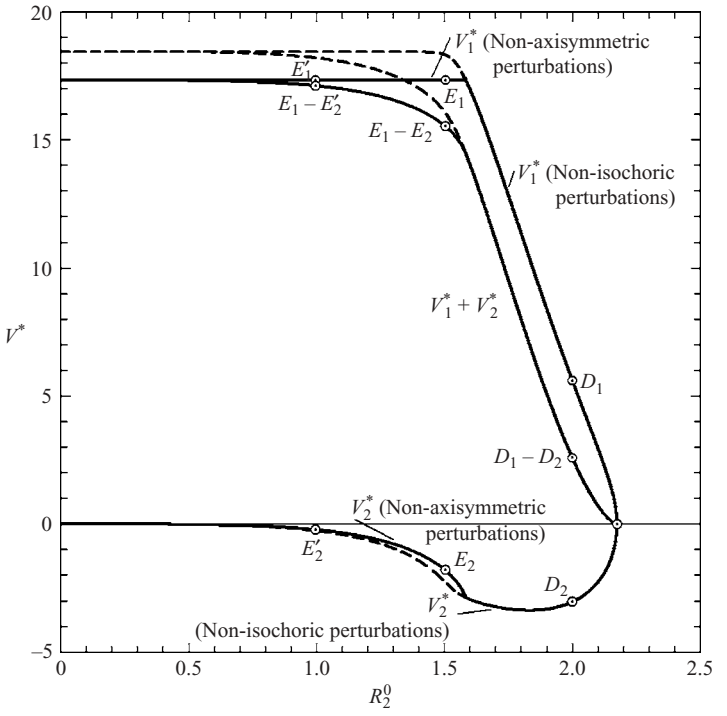

FIGURE 26. Volumes V_1^*, V_2^*, and $V_1^* + V_2^*$ for critical configurations of the systems with the larger hole radius $R_1^0 = 3.5$ as functions of the smaller hole radius R_2^0. Dashed lines correspond to states critical to non-isochoric perturbations when they cease to be the most dangerous. The point designations are the same as in figure 23.

R_1^0	H_1^*	V_1^*	Q_1^*	R_2^0	H_2^*	V_2^*	Q_2^*	$V_1^* + V_2^*$	$(Q - H)^*$
3.25	2.102	18.949	1.531	1.3118	−0.409	−1.090	−0.980	17.859	−0.571
3.30	2.016	18.853	1.465	1.4426	−0.588	−1.902	−1.139	16.951	−0.551
3.35	1.925	18.659	1.396	1.4901	−0.665	−2.294	−1.194	16.365	−0.529
3.40	1.828	18.354	1.323	1.5229	−0.705	−2.538	−1.210	15.816	−0.505
3.45	1.725	17.919	1.245	1.5527	−0.728	−2.718	−1.207	15.201	−0.479
3.50	1.613	17.331	1.162	1.5835	−0.740	−2.866	−1.191	14.466	−0.450
3.55	1.491	16.560	1.072	1.6174	−0.746	−2.997	−1.164	13.563	−0.418
3.60	1.356	15.563	0.974	1.6560	−0.745	−3.118	−1.127	12.445	−0.382
3.65	1.205	14.271	0.864	1.7021	−0.736	−3.230	−1.077	11.041	−0.341
3.70	1.029	12.577	0.736	1.7595	−0.716	−3.325	−1.009	9.252	−0.292
3.75	0.813	10.245	0.581	1.8372	−0.675	−3.371	−0.907	6.874	−0.232
3.80	0.508	6.597	0.362	1.9633	−0.569	−3.174	−0.714	3.423	−0.145

TABLE 4. Characteristic parameter values for critical systems corresponding to the crossover between non-axisymmetric and NI-critical perturbations.

6. Summary

A systematic analysis has been performed to provide a detailed discussion of the stability of two connected axisymmetric drops hanging from circular holes. Previously, only particular cases of weightless drops in contact with equal radii holes, identical

drops under non-zero gravity, and two zero-volume suspended drops with horizontal free surfaces pinned to the edges of unequal radii holes had been examined.

The collective stability of two connected drops differs significantly from that of equivalent solitary drops. This is because the classes of admissible perturbations in these cases are different. For a solitary drop, only isochoric (zero-volume change) perturbations are admissible, while for two drops the perturbations of each drop may be non-isochoric, but total liquid volume must be conserved.

This is the reason why, in general, the stability of the system of two identical drops suspended from holes of equal radii cannot be reduced to the stability of a single drop suspended from a hole of the same radius. Slobozhanin & Alexander (2003) have shown, surprisingly, that the critical volume of a single pendant drop is greater than the total critical volume of two identical drops suspended from holes of the same radius. Does this mean that the liquid volume that can be retained by surface tension in the case of a single hole is always greater than the total liquid volume that can be retained in the case of two holes with the same radius? The work presented here shows that the loss of stability of two identical drops does not lead to their rupture (although the critical perturbations are axisymmetric), but results in a continuous transition to a family of stable non-identical axisymmetric drops as the total protruded liquid volume exceeds the value critical for identical drops. The limiting quantity of the liquid that can be retained with two holes of equal radii is in fact determined by a critical system of two non-identical drops. This system is critical to axisymmetric non-isochoric perturbations, and here the total volume reaches its maximum value. Further volume increase causes the detachment of a part of liquid (the liquid dripping). Comparison of data in table 2 with volumes of critical solitary drops shows that the total protruded liquid volume that can be retained with two equal radii holes is greater than the maximum volume suspended from a single hole of the same radius if $R^0 \leqslant 1.15$. However, for $1.16 \leqslant R^0 \leqslant 2.4048$, this total volume is smaller.

An analogous continuous transition from a family of stable identical bridges to a family of stable non-identical bridges as the total liquid volume increases was detected earlier by Lowry (2000) for coupled bridges of equal length with fixed contact lines of equal radii and zero gravity. Apparently, this type of bifurcation in a point of maximum pressure is typical of systems with coupled free surfaces that may be identical. In particular, this should hold also for axial gravity (the stability limit for identical bridges can be readily drawn from the stability diagram for constant-pressure perturbations for a solitary liquid bridge obtained by Lowry & Steen, 1995). Note, however, that for non-identical drops under non-zero gravity, the stability limit is always a turning point corresponding to the maximum value of the total liquid volume. In contrast, for non-identical zero-gravity liquid bridges, the stability limit may be either a turning point (long bridges) or a pitchfork bifurcation corresponding to the loss of stability to non-axisymmetric perturbations for one of two bridges (short bridges). The latter should result in a transition to a stable family of non-axisymmetric bridges (Slobozhanin, Alexander & Resnik 1997) rather than breakage.

The more complicated case of unequal radii holes has also been examined. For zero gravity, there are two disconnected branches of stable states (see figure 5). The first branch exists for any value of the total protruded liquid volume. The second branch has a minimum value of this volume that corresponds to a system critical to non-isochoric perturbations. For non-zero gravity, three basic intervals of the larger dimensionless hole radius, R_1^0, have been established. The first is the interval $0 < R_1^0 < 2.4048$ ($R_1^0 = 0$ corresponds to weightless conditions). The presence of gravity,

results in the existence of a maximum value of the total protruded liquid volume. The previously mentioned first branch for zero-gravity conditions transforms, for given dimensionless hole radii R_1^0 and R_2^0, to a branch bounded by a state with a maximum total protruded volume. This state corresponds to a system critical to non-isochoric axisymmetric perturbations (see figure 15). The second branch of stable states may exist only for R_2^0 values that are close to R_1^0. This branch is bounded by two states that correspond to the local minimum and maximum total protruded liquid volume. These states are also critical to non-isochoric perturbations. A feature of the stable system with $R_1^0 > 2.4048$ is that it contains one pendant drop and one sessile bubble rather than two pendant drops, and there is only one branch of stable states for given R_1^0 and R_2^0. The critical system for the R_1^0 value from the interval $2.4048 < R_1^0 < 3.219$ (the second basic interval) corresponds to the maximum total protruded liquid volume and, independently of the R_2^0 value, is associated with non-isochoric critical perturbations. However, in the third interval, $3.219 < R_1^0 < 3.8317$, such stability behaviour holds only for R_2^0 values between a crossover value R_{2x}^0 and critical value, $R_{2\,cr}^0$, for the system with horizontal free surfaces. If R_2^0 is smaller than $R_{2\,x}^0$, the critical system corresponds to the drop (hanging from the larger radius, R_1^0, hole) that is critical to non-axisymmetric perturbations.

In the general case, non-isochoric (axisymmetric) perturbations are more dangerous than isochoric axisymmetric ones, and for a system of two connected drops we have to analyse only the collective stability to non-isochoric perturbations and the stability of a solitary drop (with the larger hole radius R_1^0) to non-axisymmetric perturbations.

It should be pointed out that other known coupled systems with fixed contact lines deal with zero gravity conditions and equal radii of the contact lines. These systems represent two cylindrical liquid bridges (Gillette & Dyson 1974) or the more general case of two arbitrary bridge surfaces with equal mean curvatures (Lowry 2000). In contrast to Lowry (2000), who studied the effect of disk aspect ratios on the behaviour of the coupled bridges stability, we have examined the effects of gravity and hole radii inequality on the stability of coupled drops. The study of these effects has been performed for the first time for systems with disconnected free surfaces and fixed contact lines.

A surprising feature of the stability of two connected drops strongly suggests that the stability problem for a set of $m > 2$ connected drops is far from the ultimate solution. The only result known about the stability of three connected drops relates to the zero-gravity system with spherical free surfaces pinned to edges of equal radii holes, $r_1^0 = r_2^0 = r_3^0$ (Duzaar & Steffen 1992; Wente 1999). In contrast to the case of two equal radii holes considered in § 3.2, loss of stability of three identical caps results not in a continuous transition to stable non-identical spherical caps, but in a finite jump to a stable equilibrium system consisting of two spherical caps that are less than a hemisphere and one cap greater than a hemisphere.

Hopefully, the fundamental relation between the stability of a set of connected drops to the total liquid volume conserving perturbations and the stability of individual drops involved to perturbations that satisfy the fixed liquid pressure constraint (see § 1.2) can provide some insight into the stability of $m > 2$ connected drops as in the case with two drops examined in this study.

This work was supported by National Aeronautics and Space Administration through grant NAG3-1384, and by the National Center for Space Exploration Research. L. A. S. also thanks Professor Simon Ostrach and the Case School of Engineering for support through the Wilburt J. Austin Distinguished Professorship.

REFERENCES

Adamson, A. W. 1960 *Physical Chemistry of Surfaces*. Interscience, NY.

Alexander, J. I. D. & Slobozhanin, L. A. 2004 A review of the stability of disconnected equilibrium capillary surfaces. *Microgravity Sci. Technol.* **15**, 3–21.

Babskii, V. G., Kopachevskii, N. D., Myshkis, A. D., Slobozhanin, L. A. & Tyuptsov, A. D. 1976 *Fluid Mechanics of Weightlessness*. Nauka, Moscow [in Russian].

Bashforth, F. & Adams, J. C. 1883 *An Attempt to Test the Theories of Capillary Action by Comparing the Theoretical and Measured Forms of Drops of Fluid*. Cambridge University Press.

Boucher, E. A. & Evans, M. J. 1975 Pendent drop profiles and related capillary phenomena. *Proc. R. Soc. Lond.* A **346**, 349–374.

Boys, C. V. 1902 *Soap Bubbles, Their Colors and the Forces Which Mold Them*. SPCK, London; Dover reprint, NY (1959).

Chesters, A. K. 1977 An analytical solution for the profile and volume of a small drop or bubble symmetrical about a vertical axis. *J. Fluid Mech.* **81**, 609–624.

Concus, P. 1968 Static menisci in a vertical right circular cylinder. *J. Fluid Mech.* **34**, 481–495.

Concus, P. & Finn, R. 1979 The shape of a pendant liquid drop. *Phil. Trans. R. Soc. Lond.* A **292**, 307–340.

Duprez, F. 1851 Memoire sur un cas particulier de l'equilibre des liquides. I. *Mem. Acad. R. Sci. Lett. Beaux-Arts Belgique* **26**, 42 pp. (1 plate).

Duprez, F. 1854 Memoire sur un cas particulier de l'equilibre des liquides. II. *Mem. Acad. R. Sci. Lett. Beaux-Arts Belgique* **28**, 34 pp. (1 plate).

Duzaar, F. & Steffen, K. 1992 Area minimizing hypersurfaces with prescribed volume and boundary. *Math. Z.* **209**, 581–618.

Finn, R. 1986 *Equilibrium Capillary Surfaces*. Springer.

Freud, B. B. & Harkins, W. D. 1929 The forms of the drops and determination of surface tension. *J. Phys. Chem.* **33**, 1217–1232.

Gillette, R. D. & Dyson, D. C. 1974 Stability of static configurations with applications to the theory of capillarity. *Arch. Rat. Mech. Anal.* **53**, 150–177.

Hartland, S. & Hartley, R. W. 1976 *Axisymmetric Fluid–Liquid Interfaces*. Elsevier.

Hida, K. & Nakanishi, T. 1970 The shape of a bubble or a drop attached to a flat plate. *J. Phys. Soc. Japan* **28**, 1336–1339.

Iooss, G. & Joseph, D. D. 1997 *Elementary Stability and Bifurcation Theory*. Springer.

Lonstein, Th. 1906*a* Zur Theorie des Abtropfens mit besonderer Rücksicht auf die Bestimmung der Kapillaritätskonstanten durch Tropfenversuche. *Annln Phys.* **20**, 237–268.

Lonstein, Th. 1906*b* Zur Theorie des Abtropfens. Nachtrag und weitere Belege. *Annln Phys.* **20**, 606–618.

Lonstein, Th. 1906*c* Zur Theorie des Abtropfens. Zweiter Nachtrag. *Annln Phys.* **21**, 1030–1048.

Lowry, B. J. 2000 Fixed boundary dual liquid bridges in zero-gravity. *Phys. Fluids* **12**, 1005–1015.

Lowry, B. J. & Steen, P. H. 1995 Capillary surfaces: stability from families of equilibria with application to the liquid bridge. *Proc. R. Soc. Lond.* A **449**, 411–439.

Maddocks, J. H. 1987 Stability and folds. *Arch. Rat. Mech. Anal.* **99**, 301–328.

Maxwell, J. C. 1876 Capillary action. In *Encyclopedia Britannica*. 9th edn, vol. 5, pp. 56–71. Cambridge University Press. (See also J. C. Maxwell, 1927 *The Scientific Papers*, vol. 2, pp. 541–591. Cambridge University Press).

Michael, D. H. 1981 Meniscus stability. *Annu. Rev. Fluid Mech.* **13**, 189–215.

Michael, D. H. & Williams, P. G. 1976 The equilibrium and stability of axisymmetric pendant drops. *Proc. R. Soc. Lond.* A **351**, 117–127.

Myshkis, A. D., Babskii, V. G., Kopachevskii, N. D., Slobozhanin, L. A. & Tyuptsov, A. D. 1987 *Low-Gravity Fluid Mechanics*. Springer.

Orel, V. R. 1974 Stability of an incompressible fluid acted on by surface-tension forces. Case of a doubly connected equilibrium surface. *J. Appl. Mech. Tech. Phys.* **15**, 767–774.

Padday, J. F. 1971 The profiles of axially symmetric menisci. *Phil. Trans. R. Soc. Lond.* A **269**, 265–292.

Padday, J. F. & Pitt, A. R. 1973 The stability of axisymmetric menisci. *Phil. Trans. R. Soc. Lond.* A **275**, 489–528.

Pitts, E. 1974 The stability of pendant liquid drops. Part 2. Axial symmetry. *J. Fluid Mech.* **63**, 487–508.

Pitts, E. 1976 The stability of drop hanging from a tube. *J. Inst. Math. Appl.* **17**, 387–397.

Searle, G. F. C. 1934 Mathematical discussions of problems in surface tension. In *Experimental Physics*, pp. 128–163. Cambridge University Press.

Slobozhanin, L. A. 1983 Stability of the equilibrium state of a capillary liquid with disconnected free surface. *Fluid Dyn.* **18**, 171–180.

Slobozhanin, L. A. & Alexander, J. I. D. 2003 Stability diagrams for disconnected capillary surfaces. *Phys. Fluids* **15**, 3532–3545.

Slobozhanin, L. A. & Tyuptsov, A. D. 1974 Characteristic stability parameter of the axisymmetric equilibrium surface of a capillary liquid. *Fluid Dyn.* **9**, 563–571.

Slobozhanin, L. A. & Tyuptsov, A. D. 1975 Evolution and detachment of slowly growing drops and bubbles. *J. Appl. Mech. Tech. Phys.* **16**, 83–88.

Slobozhanin, L. A., Alexander, J. I. D. & Resnik, A. H. 1997 Bifurcation of the equilibrium states of a weightless liquid bridge. *Phys. Fluids* **9**, 1893–1905.

Thompson, J. M. T. 1979 Stability predictions through a succession of folds. *Phil. Trans. R. Soc. Lond.* A **292**, 1–23.

Vaček, V. 1975 Determination of the shape of pendant drops. *Chem. Engng J.* **9**, 167–169.

Vaček, V., Nekovář, P. & Grigar, K. 1977 A simple determination of static drop shapes. In *Sb. Vysoké Školy Chem. Technol. Praze* **K12**, 125–137.

Vogel, M. J., Ehrhard, P. & Steen, P. H. 2005 The electroosmotic droplet switch: Countering capillarity with electrokinetics. *Proc. Natl Acad. Sci. USA* **102**, 11 974–11 979.

Wente, H. C. 1980 The stability of axially symmetric pendant drop. *Pacific J. Maths* **88**, 421–470.

Wente, H. C. 1989 Stability for the axially symmetric pendant drop. (Addition to Russian edn of R. Finn, *Equilibrium Capillary Surfaces* pp. 270–292. Mir, Moscow).

Wente, H. C. 1999 A surprising bubble catastrophe. *Pacific J. Maths* **189**, 339–376.